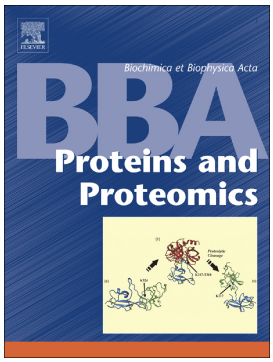

Functional characterization of methionine sulfoxide reductases from Leptospira interrogans

Natalia Sasoni, Matías D. Hartman, Sergio A. Guerrero, Alberto A. Iglesias, Diego G. Arias

PII: S1570-9639(20)30222-3

DOI: https://doi.org/10.1016/j.bbapap.2020.140575

Reference: BBAPAP 140575

To appear in: *BBA - Proteins and Proteomics*

Received date: 14 May 2020

Revised date: 17 November 2020

Accepted date: 20 November 2020

Please cite this article as: N. Sasoni, M.D. Hartman, S.A. Guerrero, et al., Functional characterization of methionine sulfoxide reductases from Leptospira interrogans, *BBA - Proteins and Proteomics* (2020), https://doi.org/10.1016/j.bbapap.2020.140575

FUNCTIONAL CHARACTERIZATION OF METHIONINE SULFOXIDE REDUCTASES FROM *Leptospira interrogans*

Natalia Sasoni[1,2#], Matías D. Hartman[1,2&], Sergio A. Guerrero[1,2], Alberto A. Iglesias[1,2] and Diego G. Arias[1,2*]

[1]Laboratorio de Enzimología Molecular - Instituto de Agrobiotecnología del Litoral (CONICET-UNL), Santa Fe, Argentina.
[2]Facultad de Bioquímica y Ciencias Biológicas - Universidad Nacional del Litoral, Santa Fe, Argentina.

[#]Present affiliation: Laboratorio de Micología y Diagnóstico Molecular. Facultad de Bioquímica y Ciencias Biológicas, Universidad Nacional del Litoral, Ciudad Universitaria – Paraje El Pozo, Santa Fe, Argentina.
[&]Present affiliation: Max Planck Institute for Biology of Ageing. Cologne, Germany.

***Corresponding author**: Diego G. Arias (darias@fbcb.unl.edu.ar). Instituto de Agrobiotecnología del Litoral (CONICET-UNL). Centro Científico Tecnológico CONICET Santa Fe. Colectora Ruta Nacional Nº 168 km 0, Santa Fe (3000), Argentina.

KEYWORDS: *Leptospira*, methionine sulfoxide reductase, redox metabolism, thioredoxin, glutaredoxin.

ABBREVIATIONS: DTNB, 5,5′-dithiobis(2-nitrobenzoic acid); DTT, dithiothreitol; Grx; glutaredoxin; GR, glutathione reductase; GSSG/GSH, glutathione disulfide/glutathione reduced; H_2O_2, hydrogen peroxide; HClO; hypoclorous acid; MBP, maltose binding protein; MetSO, methionine sulfoxide; MsrA1; methionine sulfoxide reductase A1; MsrA2: mature methionie sulfoxide reductase A2; $MsrA2_{sp}$: methionie sulfoxide reductase A2 with signal peptide; MsrB; mature methionine sulfoxide reductase B; $MsrB_{sp}$: methionie sulfoxide reductase B with signal peptide; N-AcMetSO, N-acetyl methionine sulfoxide; NBD-HCl, 7-cloro-4-nitrobenzo-2-oxa-1,3-diazole; TNB, 2-nitro-5-thio-benzoate; TrxR, thioredoxin reductase; Trx, thioredoxin.

ABSTRACT

Background

Methionine (Met) oxidation leads to a racemic mixture of *R* and *S* forms of methionine sulfoxide (MetSO). Methionine sulfoxide reductases (Msr) are enzymes that can reduce specifically each isomer of MetSO, both free and protein-bound. The Met oxidation could change the structure and function of many proteins, not only of those redox-related but also of others involved in different metabolic pathways. Until now, there is no information about the presence or function of Msrs enzymes in *Leptospira interrogans*.

Methods

We identified genes coding for putative MsrAs (A1 and A2) and MsrB in *L. interrogans serovar* Copenhageni strain Fiocruz L1-130 genome project. From these, we obtained the recombinant proteins and performed their functional characterization.

Results

The recombinant *L. interrogans* MsrB catalyzed the reduction of Met(*R*)SO using glutaredoxin and thioredoxin as reducing substrates and behaves like a 1-Cys Msr (without resolutive Cys residue). It was able to partially revert the *in vitro* HClO-dependent inactivation of *L. interrogans* catalase. Both recombinant MsrAs reduced Met(*S*)SO, being the recycle mediated by the thioredoxin system. *Lin*MsrAs were more efficient than *Lin*MsrB for free and protein-bound MetSO reduction. Besides, *Lin*MsrAs are enzymes involving a Cys triad in their catalytic mechanism. *Lin*Msrs showed a dual localization, both in cytoplasm and periplasm.

Conclusions and General Significance

This article brings new knowledge about redox metabolism in *L. interrogans*. Our results support the occurrence of a metabolic pathway involved in the critical function of repairing oxidized macromolecules in this pathogen.

1. INTRODUCTION

Bacterial species from the genus *Leptospira* were identified by 16S rRNA gene sequences in three clades: pathogenic, non-pathogenic, and another clade of undetermined pathogenicity with intermediate 16S rRNA gene sequence relatedness [1]. Among non-pathogenic (or free-living) bacterium is *L. biflexa* serovar Patoc which can be found in wet environments and surface water. Contrary, *L. interrogans* serovar Icterohaemorrhagiae or Cophenageni is in a pathogenic clade, and it could survive in different environments (from the soil and water to the mammalian host's tissues) and is the etiologic agent of human leptospirosis [2]. Therefore, Leptospirosis is an infectious disease caused by pathogenic leptospires that are transmitted (directly or indirectly) by contact with the urine of infected animals (mainly, rats) to humans, thus being a zoonosis (WHO, https://www.who.int/home). This infection frequently results in a hard life-threatening illness characterized by liver dysfunction, kidney failure, and pulmonary hemorrhage [3]. Like other infectious agents, the survival of *L. interrogans* depends on its ability to evade the oxidative killing mediated by host cells (including macrophages). Until now, little information is available concerning mechanisms for functional antioxidant proteins present in this pathogen. The bibliography describes the presence of catalase in abundant concentration localized in the bacterial periplasmic space [4], a typical 2-Cys peroxiredoxin (AhpC) [5], and the thioredoxin system [6]. However, in contrast to other pathogenic bacteria, no information about repairing oxidized enzymatic systems was reported in *Leptospira interrogans*.

In general, oxidative and nitrosative changes of specific amino acid residues are major processes for protein posttranslational modification, with significant physiological and pathological consequences. In this regard, Met oxidation is a posttranslational modification that occurs *in vivo* under normal or stress conditions leading to a racemic mixture of *R* and *S* forms of MetSO [7]. Particularly, Met residue has high reactivity to HClO, a reactive halogen species generated in pathological conditions [7, 8]. The MetSO derivatives are reduced by a group of enzymes called methionine sulfoxide reductases (Msr). At present, six classes of Msrs were described in several organisms. Three Mo-dependent (metalloproteins) bacterial Msr-like enzymes (MsrP, DmsA, and BisC) [9], and three thiol-dependent Msr enzymes (MsrA, MsrB, and MsrC) [10-12]. MsrA and MsrB were found in organisms from almost all living kingdoms [9, 13-20]. MsrA reduces with high specificity the *S* isomer of MetSO (free or in proteins), while

MsrB is specific for reducing the *R* isomer (mainly in proteins) [10-12]. Besides, MsrC (or *f*Msr, for "*free*"-methionine sulfoxide reductase), mainly found in unicellular organisms, is responsible for the specific conversion of free L-Met(*R*)SO [21-23]. The active sites of both Msrs are adapted for binding protein-bound methionine sulfoxide (L-MetSO) more efficiently than free L-MetSO. Besides, thiol-dependent Msrs are structurally unrelated enzyme classes, but they share the same chemical mechanism implying sulfenic acid chemistry, representing a case of convergent evolution [9, 11, 12]. The thiol-dependent Msrs can be classified according to the kinetic mechanism employed to recycle the catalytic Cys [11, 24]. The primary physiologic reductants of thiol-dependent Msr are Trx (except for 1-Cys Msrs) and Grx [12, 25, 26]. The latter possess higher catalytic efficiency to reduce 1-Cys Msrs than 2-Cys or 3-Cys Msrs [12, 25, 26].

Available MsrA structures indicate a structurally well conserved active site containing the consensus sequence GCFW(G/H) located at the N-terminus and include the catalytic Cys [11]. However, differences in structure are evident in the C-terminal region harboring the resolving Cys [11]. Regarding MsrBs, a structural characteristic is the presence of a metal-binding site composed of two CXXC motifs. It is located on the opposite side of the active site and binds a zinc atom [11, 27]. There is inconclusive evidence regarding the role of the metal within the protein: whereas some authors argue that it can modulate MsrB catalytic efficiency [27], others claim that metal ion substitution does not affect the protein activity [28].

In different pathogenic bacterium such as *Enterococcus faecalis* [29], *Campylobacter jejuni* [30] and *Pseudomonas aeruginosa* [31], Msrs are essential for oxidative and nitrosative stress protection and bacterial virulence. Besides this, mainly in human, the Msrs have also been involved in some physiological regulation of protein function, making Met oxidation similar to other reversible posttranslational modification [32]. The last finding highlights a new era in the understanding of Msr function and should facilitate further studies on the physiological role of Msrs [33].

In this work, we presented the recombinant expression of three genes coding for putative Msrs (*linmsra1*, *linmsra2*, and *linmsrb*) from *Leptospira interrogans.* We performed biochemical studies and analyzed the different functional properties of these proteins. The data here presented contributing to general redox metabolism understanding of *L. interrogans.*

2. MATERIALS AND METHODS

2.1. *Materials*

Bacteriological media were purchased from Britania Laboratories and BD Biosciences (Argentina). *Pfu* DNA polymerase, *Taq* DNA polymerase, and restriction enzymes were purchased from Promega (Argentina). Amylose-resin was acquired from New England Biolabs. Hi-Trap column and Superdex-200 were purchased from GE-Healthcare (Argentina). The monoclonal anti-His-tag antibody, racemic L-MetSO, and all other reagents and chemicals were of the highest quality commercially available from Sigma-Aldrich (Argentina) or similar. The separation of the L-MetSO isomers was carried out following the method of Lavine [34] from the pure L-MetSO racemic mixture by differential precipitation with picric acid and methanol. Under our conditions, we obtained a purity greater than 99% for the L-Met(*S*)SO isomer and a purity of 90% for the L-Met(*R*)SO isomer [the remaining 10% corresponds to the L-Met(*S*)SO isomer].

2.2. In vitro *culture of* Leptospira interrogans

L. interrogans serovar Copenhageni strain Fiocruz L1-130 cells were grown in EMJH medium (Ellinghausen-McCullough-Johnson-Harris), a BSA-Tween80 medium (pH 7.4) in static culture for 3-5 days at 28 °C [35, 36]. The cell density was recorded at 420 nm in an S-26 spectrophotometer (Boeco-Germany). Bacteria number was estimated according to the relation established for Louvel et al [37] where $OD_{420\ nm}$ of 1 represents $2.1 \cdot 10^9$ bacteria ml^{-1}.

Cell extracts were produced from biomass pools of three biological replicates (obtained from exponential phase cultures of *L. interrogans* in EMJH medium). The cellular pellet was suspended with 1 ml of 100 mM potassium phosphate buffer pH 7.0, 2 mM EDTA. Cell lysis was performed through three cycles of freezing (at -80 °C) and thawing (at 37 °C), followed by sonication. The cell lysate was centrifuged at 21,000 *xg* for 30 min at 4 °C. The soluble protein-extract (supernatant) obtained was used for enzymatic activity determination.

2.3. *Bacteria and plasmids*

Escherichia coli TOP10 F´ (Invitrogen) and *E. coli* BL21 (DE3) (Novagen) cells were utilized in routine plasmid construction and expression experiments, respectively. The vector pGEM-T Easy (Promega) was selected for cloning and sequencing purposes.

The expression vectors were pET22b (Novagen), pMAL-C-TEV (kindly provided by Dr. Wulf Blankenfeldt from the Helmholtz Center for Infection Research, Germany), and pCold-I (Takara Bio Inc.). Genomic DNA from *L. interrogans* was obtained using the Wizard Genomic DNA Purification Kit (Promega). DNA manipulation, *E. coli* cultures, and transformation were performed according to standard protocols [38].

2.4. *Molecular cloning of msra1, msra2, msra2$_{SP}$, msrb, and msrb$_{SP}$ genes*

Based on available information about *L. interrogans* serovar Copenhageni strain Fiocruz L1-130 (http://meta.microbesonline.org/ and http://bioinfo03.ibi.unicamp.br/leptospira/) genome sequences, *msra1, msra2* (the ORF encoding for mature MsrA2), *msra2*$_{SP}$ (the ORF encoding for MsrA2 with signal peptide), *msrb* (the ORF encoding for mature MsrB) and *msrb*$_{SP}$ (the ORF encoding for MsrB with signal peptide) genes were amplified by PCR. Each PCR was performed using genomic DNA and specific primer pairs (Table 1) under the following conditions: 95 °C for 10 min; 30 cycles of 95 °C for 1 min, 55-65 °C for 1 min 72 °C for 1 min, and 72 °C for 10 min. The PCR products were subsequently purified and ligated into pGEM-T Easy vector and its fidelity and identity were confirmed by complete DNA sequencing (Macrogen, South Korea).

The obtained pGEM-T Easy constructions were digested with appropriate restriction enzymes (Table 1) and the purified ORFs were ligated to different expression vectors using T4 DNA ligase (Promega) for 16 h at 4 °C. The *linmsrb*$_{SP}$ and *linmsrb* genes were cloned in pET22b plasmid. The *linmsra1* gene was cloned in the pCold-I plasmid (using the *Bam*HI/*Sal*I restriction sites). Finally, the *linmsra2*$_{SP}$ and *linmsra2* genes were cloned in the pET22b (using the *Nde*I/*Xho*I restriction sites), pCold-I (using the *Bam*HI/*Sal*I or *Nde*I/*Sal*I restriction sites), and pMAL-C-TEV plasmids (using the *Nde*I/*Xho*I restriction sites). Competent *E. coli* BL21 (DE3) cells transformed with the construct were selected in agar plates containing Lysogeny Broth (LB; 10 g l^{-1} NaCl, 5 g l^{-1} yeast extract, 10 g l^{-1} peptone, pH 7.4) supplemented with ampicillin or kanamycin (50 μg ml^{-1}) as appropriate. Preparation of plasmid DNA and subsequent restriction treatment were performed to check the correctness of the construct.

The sequences coding for *Lin*MsrA1C25S and *Lin*MsrA2C18S proteins were generated following the instructions of the commercial protocol for QuikChange® Site-Directed Mutagenesis kit (Stratagene) with some technical adaptations. Briefly, we designed two entirely complementary primers containing the nucleotide with the desired mutation in

the center of these primers (Table 1). PCR mix was performed using as template 10 ng of pGEM-T Easy/*Lin*MsrA1 or pGEM-T Easy/*Lin*MsrA2 plasmids purified from *E. coli* TOP10 F´ with DNA methylase activity, 1 μM primers, 0.2 mM dNTPs, and 2.5 U *Pfu* DNA polymerase (Fermentas). The PCR reaction conditions were: 94 °C for 5 min; 12 cycles of 94 °C for 1 min, 55 °C for 1 min, and 72 °C for 11 min. After PCR, the amplified product was treated for 3 h at 37 °C with 10 U of *Dpn*I restriction enzyme (Fermentas), which can degrade the parental methylated DNA plasmid. Then, *E. coli* TOP10 F′ competent cells were transformed with the *Dpn*I digested plasmid, and the recombinant clones were selected to verify the mutation by sequencing.

2.5. *Overexpression and purification of recombinant proteins*

A single colony of *E. coli* BL21 (DE3) transformed with each recombinant plasmid was selected. Overnight cultures were diluted 1/100 in fresh LB medium (for *Lin*MsrAs expression) or M9 medium [28] (without or with addition of 100 μM of $CoCl_2$, $ZnCl_2$ or $FeCl_2$ for *Lin*MsrB expression) supplemented with the appropriate antibiotic and growth under identical conditions to exponential phase, $OD_{600\ nm}$ of 0.6. The induction of expression of the respective recombinant proteins was performed with 0.25 mM IPTG for 16 h at 25 °C. Then, the cells were harvested and stored at -20 °C until further use. Purification of each recombinant protein was performed using Hi-Trap™ chelating HP (GE Healthcare). Briefly, the bacterial pellet was re-suspended in binding buffer (20 mM Tris-HCl pH 7.5, 400 mM NaCl, and 10 mM imidazole), and then disrupted by sonication. Centrifugation (20,000 *xg* for 30 min) of the lysate allowed removing cell debris. The resultant crude extract was loaded onto a column already equilibrated with binding buffer. After being washed with 10 volumes of the same buffer, the recombinant proteins were eluted with elution buffer (20 mM Tris-HCl, pH 7.5, 400 mM NaCl, 300 mM imidazole). Also, *Lin*MsrA2 and *Lin*MsrA2C18S obtained from the IMAC chromatography (as an MBP-fusion protein) were treated with TEV protease (at a ratio of 1 μg protease to 100 μg of recombinant protein at 8 °C for 16 h in 100 mM Tris-HCl pH 8.0 and 1 mM DTT) followed by amylose affinity chromatography (New England Biolabs), according to the manufacturer's instructions. Fractions containing pure protein were pooled, concentrated, and frozen with 20% (v/v) glycerol at -80 °C. Catalase, TrxR, and Trx from *L. interrogans* were recombinantly expressed and purified as described elsewhere [4, 6].

2.6. *Protein methods*

Protein electrophoresis was carried out under denaturing conditions (SDS– PAGE) as described in [39]. For non-reducing SDS–PAGE, the samples were prepared with buffer without reducing agent. Protein concentration was determined following the procedure described by Bradford [40] using bovine serum albumin (BSA) as standard.

The molecular mass of the recombinant proteins at their native functional states was determined by gel filtration chromatography using a Superdex 200 column (GE Healthcare) equilibrated with 50 mM HEPES buffer pH 8.0 containing 100 mM NaCl and 0.1 mM EDTA, at a flow rate of 1 ml min^{-1}. A calibration curve was constructed by plotting the log_{10} of the molecular mass vs. the distribution coefficient (K_{av}) measured from standard proteins (thyroglobulin, 669 kDa; ferritin, 440 kDa; aldolase, 158 kDa; conalbumin, 75 kDa; ovalbumin, 43 kDa; carbonic anhydrase, 29 kDa; ribonuclease A, 13.7 kDa; and aprotinin 6.5 kDa).

Protein thiol and sulfenic acid groups were quantified with 5,5dithiobis2nitrobenzoic acid (DTNB, $\varepsilon_{412\ nm}$ = 14.15 $mM^{-1}cm^{-1}$[41]) or 7-chloro-4-nitrobenzo-2-oxa-1,3-diazole (NBD-HCl, ε_{340nm} = 13.4 $mM^{-1}cm^{-1}$,[42, 43]) respectively, in 100 mM Tris-HCl pH 7.5 at 25 °C.

MetSO-rich *L. interrogans* protein extracts were obtained from washed cells (~10^{10} cell·ml^{-1}, in exponential phase growth) that were incubated in the absence and presence of 100 μM HClO for 30 min in PBS buffer at 28 °C. Subsequently, the cells derived from each treatment were disrupted by sonication in the presence of a lysis solution (50 mM potassium phosphate, pH 8.0, 0.1% (v/v) NP-40, 1 mM EDTA, and 100 mM iodoacetamide) supplemented with protease inhibitor cocktail (SETIII, Calbiochem). Then, the crude extracts were obtained by centrifugation (20,000 *xg* for 30 min at 4 °C), and a differential precipitation treatment with ammonium sulfate at 30% saturation (to remove membranes and DNA by precipitation) was applied to the resulting supernatants. After centrifugation, the obtained supernatants were treated with 100 mM DTT for 15 min at 30 °C. Next, the samples were desalted using BioGel spin-columns (equilibrated with 50 mM potassium phosphate, pH 8.0, and 1 mM EDTA). Finally, the proteins were treated again with 100 mM iodoacetamide for 15 min at 30 °C and desalted using spin columns (equilibrated with 50 mM TRIS-HCl, pH 7.5, and 1 mM EDTA). The objective of the treatment (reduction and subsequent alkylation) of the total protein extracts is to eliminate all potentially reactive forms of cysteine residues

(oxidized forms, such as disulfides, sulfenic acids, or nitrosothiols), which could interfere in the assay for activity (Trx or Grx-dependent coupled assay system). The resulting protein extracts were used to evaluate the activity of MsrAs and MsrB using Trx or Grx (as a reducing substrate) to reduce protein MetSO (see 2.10).

2.7. *Antibodies production and immunodetection*

Serums against MsrB and Lp32 [44] (a surface Lipoprotein) from *L. interrogans* were raised in rabbits immunized with the purified recombinant protein, as previously described [45]. Rabbit anti-*Trypanosoma cruzi* MsrA (anti-*Tcr*MsrA), prepared as described previously [46], was used to detect *Lin*MsrA proteins. Proteins (recombinant or protein extracts) in SDS-PAGE gels were blotted onto nitrocellulose membranes using a Fast Blot, Semi-Dry Electrophoretic Transfer apparatus (Biometra GmbH). The membrane was blocked with 4% (w/v) skimmed milk in PBS for 1 h at room temperature, subsequently incubated at room temperature for 1 h with the primary antibody, and then with HRP-conjugated anti-rabbit secondary antibodies for 1 h at room temperature. The ECL western blotting detection reagents (Thermo Scientific) served to visualize the bands.

2.8. *Digitonin titration assays*

A cellular pellet from a culture of 24 ml of *L. interrogans* (in the exponential growth phase) of $OD_{420\,nm} = 0.23$ was treated successively with increasing concentrations of digitonin (from 0 to 4 mg ml^{-1}) in extraction buffer (20 mM Tris-HCl, 100 mM NaCl, 1 mM EDTA and 250 mM sucrose, pH 7.5). Protein fractions in the supernatants were subjected to SDS-PAGE and western blot analysis. Polyclonal antibodies against *Lin*TrxR [6] and *Lin*AhpC [5] were cytoplasmic markers and *L. interrogans* catalase (*Lin*catalase), a periplasmic marker [4].

2.9. *Determination of metal cofactors in protein*

The quantification of metal atoms (Fe, Zn, Cu, or Co) present in the pure recombinant proteins was performed using atomic absorption spectrophotometry at the SECEGRIN facility (CCT-CONICET Santa Fe, Argentina). The effective concentration of active enzyme was estimated based on the [metal atom]/[*Lin*MsrB] ratio.

2.10. *Enzyme activity assay*

All the enzymatic assays were performed, unless otherwise indicated, at 30 °C, in a final volume of 50 µl using a Multiskan Ascent one-channel vertical light path filter photometer (Thermo Electron Co). The data were plotted as initial v·[enzyme]$^{-1}$ (min^{-1}) versus substrate concentration (µM), and the kinetic constants acquired by fitting the records with nonlinear least-squares formula and the Michaelis-Menten equation. Kinetic constants were the means of at least three independent sets of data.

The MetSO reductase activity was measured monitoring the NADPH oxidation at 340 nm. *Homo sapiens* glutaredoxin 1 (*Hsa*Grx, form Sigma-Aldrich - G5298) or *Lin*Trx were tested as electron donor from the Msrs. The reaction mixture was composed by 100 mM potassium phosphate, pH 7.0, 2 mM EDTA, 200 µM NADPH, 2 µM *Lin*TrxR or 1 U ml^{-1} *Sacharomyces cerevisiae* glutathione reductase (Sigma-Aldrich - G3664); 20 µM *Lin*Trx or 25 µM *Hsa*Grx (plus 3 mM GSH), and different concentrations of *Lin*MsrA1 (from 0.01 to 10 µM), *Lin*MsrA2 (from 0.01 to 10 µM), *Lin*MsrA1C25S (from 2 to 125 µM), *Lin*MsrA2C18S (from 10 to 100 µM) or *Lin*MsrB (from 0.1 to 150 µM). The measurements were started by adding 5 mM of L-MetSO or N-AcMetSO. Steady-state kinetics analysis was performed using 0.1 to 5 mM L-MetSO or N-AcMetSO, 0.1 to 40 µM *Lin*Trx or *Hsa*Grx (plus 3 mM GSH) and 1 µM *Lin*MsrA1, or 1 µM *Lin*MsrA2, or 12 µM *Lin*MsrA1C25S, or 10 µM *Lin*MsrB. The kinetic constants were acquired by fitting the data with a nonlinear least-squares formula and the Michaelis–Menten equation. Kinetic constants are the mean of at least three independent sets of data.

The specificity of L-MetSO isomer reduction by *Lin*Msrs was evaluated using a reaction mixture of 100 mM potassium phosphate, pH 7.0, 10 mM DTT, 1 mM L-MetSO or L-Met(*R*)SO or L-Met(*S*)SO, and 10 or 100 µM of each one recombinant protein. The reaction mixture was incubated at 37 °C for 1-2 h and then was loaded on silica sheets (TLC ALUMINIUM plates, Merck) for thin-layer chromatography (TLC). The mobile phase was a solution of butanol: acetic acid: water (60:15:25). The chromatogram was revealed by ninhydrin spray [47].

The reduction of the sulfenic acid form of *Lin*MsrB (*Lin*MsrB-SOH) was evaluated by monitoring the decreased concentration of 2-nitro-5-thio-benzoate (TNB) at 405 nm. The reaction mixture contained 200 mM Tris-HCl pH 8.0, 2 mM EDTA, 200 µM TNB and different concentrations of *Lin*MsrB (0, 25, 50 or 100 µM). The reaction was started

with 5 mM L-MetSO. The synthesis and purification of TNB were produced according to [48].

Catalase activity was monitored by H_2O_2 consumption at 240 nm in an S26 spectrophotometer (Boeco-Germany) at 25 °C. The reaction mixture comprised 100 mM potassium phosphate, pH 7.0, 0.1 to 1 nM *Lin*catalase and 10 mM H_2O_2 in a final volume of 1 ml [49]. The activity was calculated using the molar extinction coefficient of 40 mM^{-1} cm^{-1}.

2.11. *Yeast complementation assays*

In vivo activity of the *Lin*Msrs was checked using the triple *msr* deletion mutant GY202 (*ΔmsraΔmsrbΔfrmsr*) and W303-1B (parental strain) [50]. The *Saccharomyces cerevisiae* GY202 strain was transformed with parental plasmid p425GPD (abbreviated as p425, as negative control), p425–*linmsra*1, p425-*linmsra*2 or p425-*linmsrb* and selected for leucine auxotrophy on SD-agar medium supplemented with L-Met [51]. For the complementation assay, each recombinant clone was cultivated on the SD-agar medium supplemented with 100 µM L-Met, L-Met(*S*)SO, or L-Met(*R*)SO at 28 °C until growth was visualized. For oxidative stress assays, cellular suspensions ($5 \cdot 10^6$ cell ml^{-1}) were incubated at 28 °C for 1 h with or without oxidant compounds: 0.1 or 1 mM H_2O_2 or 0.1 mM HClO. After this time, serial dilutions (1/5) of each culture were performed, and 5 µl of each dilution was plated and incubated at 28 °C until observing yeast development.

2.12. *Molecular modeling*

Structural models of *Lin*Msrs were generated by homology modeling using the Modeller v9.20 program [52], with structure optimization algorithms. *Lin*MsrAs models were based on the resolved structure of MsrA from *E. coli* (PDB 1FF3), and *Populus trichocarpa* (PDB 2J89). *Lin*MsrB models were based on the solved structure of MsrB from *Methanothermobacter thermautotrophicus* (PDB 2K8D), *Neisseria meningitidis* (PDB 3HCG), and *Burkholderia pseudomallei* (PDB 3CXK). Sequences alignment was carried out using the Clustal X algorithm with the program Bioedit v7.0.8 (Ibis Bioscience 2007). The structures were evaluated using the program online Verify 3D (http://nihserver.mbi.ucla.edu/Verify_3D/), and the best-obtained models were visualized for their analysis using UCSF Chimera (https://www.cgl.ucsf.edu/chimera/).

2.13. *Phylogenetic trees*

MsrAs and MsrBs sequences were downloaded from the NCBI database (including bifunctional MsrAB proteins) and used to generate multiple alignments (Supplementary data - Table 1 and Table 2). The Gblock (Castresana lab) served to eliminate poorly aligned positions and divergent regions Tree reconstruction was performed with Seaview 4.4 [53] using the Neighbor-Joining method and a bootstrap of 10,000. The tree was prepared in the FigTree 1.4 program (http:// tree.bio.ed.ac.uk/).

3. RESULTS

3.1. In silico *analysis of the sequences coding for Msrs and recombinant expression*

In the analysis of the *L. interrogans* genome, we could identify a sequence coding for an MsrB protein (NCBI, WP_000790973.1, and UNIPROT, M3G797_LEPIT). Fig. 1 shows an amino acid sequence alignment of the full sequence of *Lin*MsrB (*Lin*MsrB$_{SP}$) with homologous enzymes from different organisms. *Lin*MsrB$_{SP}$ contains four Cys residues in conserved positions related to the metal atom binding and a fifth residue involved in catalysis. We analyzed MsrBs in a phylogenetical context, as well. An in-depth analysis of the protein sequences in combination with the phylogenetic separation allowed us to identify four different clades that could be related to the presence of the Cys residues related to the metal atom binding (and the specific sequences) or the absence of such residues (Fig. 2). The largest clade (violet lines) is constituted by archaea, cyanobacteria, acidobacteria, proteobacteria (a, e and g), fungi, plants, the protist *T. cruzi*, and the *L. interrogans* MsrB sequences. Within this group, except for g- and e-proteobacteria, all the proteins contain the consensus sequence CA(G/A)C as part of the first CXXC motif. A second small group (turquoise lines) is comprised of b-, d-proteobacteria, and cyanobacteria with a consensus motif CI(G/C)C. The second largest group is formed by three different subgroups: the proteins containing the motif CVCC (yellow lines), those containing the CL(V/I)C motif (red lines), and a mixed group of MsrB and MsrAB proteins that are non-metal binding (grey lines). The CVCC clade (yellow lines) group the protein sequences of *L. biflexa* and animals (namely human, mouse and Xenopus) whereas the CL(V/I)C clade (red lines) is composed of d-proteobacteria. The non-metal binding protein sequences (gray lines) group only prokaryotic sequences; proteobacteria, archaea, and firmicutes. This clade is formed by both MsrBs and MsrABs sequences.

Interestingly, the sequence of *Lin*MsrB$_{SP}$ presents a non-conserved N-terminal extension containing two Cys residues (at positions 13 and 19). Hypothetically, these residuals could act as non-conserved putative resolving Cys for catalytic Msr activity. Given this and as part of the analysis to predict a possible function of this N-terminal, we performed an *in silico* analysis using the online predictors SOSUI and SignalP (Supplementary data – Fig. 1). Such predictions suggested that the non-conserved N-terminal extension of *Lin*MsrB$_{SP}$ corresponds to a signal peptide. In parallel, we performed a domain conservation search using the NCBI database (https://www.ncbi.nlm.nih.gov/Structure/cdd/wrpsb.cgi?). The *in silico* analyzes suggest that the SelR domain of the protein starts at Tyr^{38} (data not shown). Alternatively, we observed that in the UNIPROT database is presented a shorter MsrB sequence from *L. interrogans* (serogroup Icterohaemorrhagiae serovar copenhageni, Q72NN2 MSRB_LEPIC). This short sequence lacks the first 35 amino acids of the N-terminal that is present in *Lin*MsrB$_{SP}$. Given these observations, we cloned the full sequence and a truncated sequence (omitting the 105 bp of the 5'-end). The resulting mature protein (*Lin*MsrB) has 131 amino acids (15 kDa), whereas the full-length recombinant protein (*Lin*MsrB$_{SP}$, including the signal peptide) is a protein of 166 amino acids (18.5 kDa).

The expression assay in *E. coli* BL21 (DE3) showed a higher abundance in the soluble fraction for pET22b/*Lin*MsrB than pET22b/*Lin*MsrB$_{SP}$ (Supplementary data - Fig. 2A). Interestingly, western blot using anti-*Lin*MsrB allowed us to detect two bands in total soluble fraction from full sequence over-expressing cells. Each band corresponding with the *Lin*MsrB$_{SP}$ and *Lin*MsrB forms (Supplementary data - Fig. 2A). This observation suggests that the complete form of the protein is processed proteolytically (probably after translocation to the periplasm in *E. coli*). To evaluate this proposal, we carried out a subcellular fractionation of *E. coli* that over-expresses both the complete form (*Lin*MsrB$_{SP}$) and the truncated form (*Lin*MsrB, the putative mature form, without the coding sequence for the signal peptide). We performed a periplasmic-enrichment from *E. coli* BL21 (DE3) cells transformed with pET22b/*Lin*MsrB$_{SP}$ or pET22b/*Lin*MsrB construction, following the osmotic shock method as is described by [54]. With the fractions, cytoplasmic and enriched-periplasmic, we performed western blot assays using anti-*Lin*MsrB and the recombinant protein (*Lin*MsrB) as a molecular marker. As shown in Supplementary data - Fig. 2B, for *E. coli* BL21 (DE3) containing pET22b/*Lin*MsrB$_{SP}$ plasmid, the expression was detected both in the cytoplasmic and the enriched-periplasmic fractions. Interestingly, the variant detected in the periplasmic

fraction has an identical migration pattern regarding the recombinant *Lin*MsrB (without the first 35 amino acids from the full version) in the highest proportion than the full version (*Lin*MsrB$_{SP}$) detected in the cytoplasm. This result suggests that the N-terminal of *Lin*MsrB$_{SP}$ is a functional peptide in *E. coli* and that this protein is processed by *E. coli* proteolytic machinery (losing both Cys^{13} and Cys^{19} from the full sequence, the potential candidate residues for resolutive Cys), resulting in the accumulation of the mature form in the periplasm of the bacterium. Contrary, *E. coli* BL21 (DE3) transformed with pET22b/*Lin*MsrB, showed only an abundant expression band in the cytoplasmic fraction. Because of these results, and the higher yield obtained as a processed form of the protein, we continued the studies using the construct pET22b/*Lin*MsrB that codes for the mature form and perform the functional characterization.

In addition to MsrB, two putative coding sequences for MsrA proteins (*linmsra1*, LIC10545, and *linmsra*2, LIC12978) were identified in the genome project of *L. interrogans* (http://aeg.lbi.ic.unicamp.br/world/lic/). The full sequence genes code for proteins of 188 (*linmsra1*) and 198 (*linmsra2)* amino acids, with theoretical molecular masses of 21 kDa and 23 kDa, respectively. Fig. 3 illustrates an alignment of the amino acid sequences of full sequence *Lin*MsrA1 and *Lin*MsrA2 in comparison with MsrA from different sources. *Lin*MsrAs exhibited similar identity (~37%) to humans, *Bos taurus*, and bacteria counterparts, and they contain the characteristic redox-active motif GCFWC. This structural characteristic was observed in the MsrA enzyme from *Bacillus subtilis* [11]. The presence of this vicinal Cys residue in the active site of *Lin*MsrAs, allows us to hypothesize that at this residue is a putative resolutive Cys (the catalytic and a possible resolutive Cys are vicinal residues). In addition to the Cys within the CXXC motif, *Lin*MsrA1 has three further Cys residues, while *Lin*MsrA2 has only one extra Cys residue (see positions marked by arrows in Fig. 3). Furthermore, we analyzed the *Lin*MsrAs in a phylogenetic context to construct a tree composed of thirty-seven sequences, including all the living kingdoms. As can be observed in Fig. 4, two main clades can be distinguished: the first one comprising five prokaryotic MsrAB sequences and the second and larger one comprised of MsrA sequences. The MsrAB clade contains proteins that harbour the GCFWG motif (red lines). Conversely, the MsrA clade is further separated into three different groups: i) a group comprised of fungi, *T. cruzi*, and a-proteobacteria proteins containing a GCFWG motif (red lines); ii) a group comprised of both eukaryotic (animalia and plantae sequences) and prokaryiotic (a-, g-

proteobacteria, cyanobacteria, and actinobacteria) GCFWG-containing proteins and iii) a group of prokaryotic sequences containing the motif GCFWC (turquoise lines) and formed by archaea, b- and d-proteobacteria, cyanobacteria, firmicutes, and the spirochaetes *L. interrogans* and *L. biflexa*. It is worth mentioning that *Lin*MsrA1 (sequence number 8) clustered with other spirochaetes like *L. biflexa* (sequence number 7), contrary to *Lin*MsrA2 that groups with Msrs from Firmicutes (sequences number 15-17) and other prokaryotes, namely *Desulfovibrio vulgaris* (sequence number 11) and the cyanobacterium Synechococcus elongatus (sequence number 20).

Interestingly, in a similar way to *Lin*MsrB, the full sequence of *Lin*MsrA2 presents a non-conserved N-terminal extension. *In silico* analysis using the online predictors SOSUI and Signal-P (Supplementary data – Fig. 3) predicted that the initial 21 amino acids (average) of the full sequence of *Lin*MsrA2 correspond to a signal peptide (with a high probability of proteolytic cut at position 21-22). Given this observation, we performed a strategy similar to the one carried out for *Lin*MsrB. We cloned the full sequence and a truncated sequence (omitting the 57 bp of the 5'-end). As a result, the full-length recombinant protein (*Lin*MsrA2$_{FL}$, including the signal peptide) is a protein of 198 amino acids (23 kDa) whereas the mature protein (*Lin*MsrA2) has 179 amino acids (21 kDa). No expression of these cloned MsrA1 sequences was detected using pET22b or pCold-I plasmids (by SDS-PAGE and western blot assays using anti-*Trc*MsrA antibodies and/or monoclonal anti-His tag antibody, data not shown). Given these results and the observed data for *Lin*MsrB, we cloned the coding sequence of the mature version of the protein (without the first 19 amino acids, *Lin*MsrA2) in the pMAL-TEV plasmid, where we could detect the recombinant expression of the protein as a fusion to 6His-MBP.

In summary, regarding recombinant protein production, each cloned gene was expressed in *E. coli* BL21 (DE3) cells to produce the respective recombinant protein fused to an N-terminal 6Histag (*Lin*MsrA1 and *Lin*MsrA1C25S), C-terminal 6Histag (*Lin*MsrB) or 6His-MBP (*Lin*MsrA2 and *Lin*MsrA2C18S). The analysis by SDS-PAGE showed that the recombinant enzymes were produced and purified with ~98% purity (data not shown). These proteins were stored at -80 °C without loss of activity for at least eight months.

3.2. *Functional characterization of* Lin*Msrs* in vitro *and* in vivo

We performed an *in vitro* assay to determine the ability of *Lin*MsrB, *Lin*MsrA1, and *Lin*MsrA2 to reduce non-peptide MetSO. Specifically, we evaluated the capacity of the purified recombinant proteins to catalyze the reduction of the different isomers of L-MetSO using DTT as a reductant. After that, the reaction products were resolved by TLC using ninhydrin as a chromogenic reagent. As shown in Fig. 5, the conversion of L-MetSO to L-Met was partial when the reaction mixture was composed of L-Met(*R*)SO and *Lin*MsrB (lane 8), whereas no L-Met was generated when the enzyme was incubated with L-Met(*S*)SO (lane 9). Besides, the presence of L-Met was detected in reactions containing both *Lin*MsrA1 and *Lin*MsrA2 plus the L-Met(*S*)SO isomer (lanes 13 and 15), but the result was negative for the L-Met(*R*)SO isomer (lanes 12 and 14). It should be noted that the low-intensity spot in the Met position observed in the latter condition is because the L-Met(*R*)SO isomer is not completely pure (as was pointed out in Material and Methods).

To evaluate *Lin*Msrs functionality *in vivo*, we performed yeast complementation assays. The open reading frame of each Msr was cloned into the p425 vector [51] and introduced into *S. cerevisiae* GY202 cells (deletion mutant for the three Msr enzymes) [50]. As can be observed in Fig. 6, the *S. cerevisiae* GY202 strain complemented with *Lin*MsrA1, *Lin*MsrA2, and *Lin*MsrB, developed in the presence of L-Met similarly to the negative control. However, when L-MetSO replaced L-Met, proliferation was only observed in those yeast strains complemented with the transgenes. Also, using the SD-agar medium supplemented with L-Met(*S*)SO, only the cells transformed with the encoding genes for *Lin*MsrA1 and *Lin*MsrA2 could grow. Conversely, the cells that expressed *Lin*MsrB grow in the SD-agar medium with racemic L-MetSO but not in the presence of L-Met(*S*)SO (Fig. 6). These results indicated that these proteins are actual L-MetSO reductases *in vivo.* These results support the stereospecificity of this type of enzymes, previously observed by the *in vitro* assays shown in Fig. 5.

Additionally, we analyzed the oxidative stress sensitivity of the different recombinant yeasts. Cell suspensions were incubated 1 h at 28 °C without oxidant or in the presence of either H_2O_2, (0.1 and 1 mM), or 0.1 mM HClO and then plated on SD-agar. The p425 construct was used to transform *S. cerevisiae* W303-1B (parental), and GY202 (triple mutant) strains used as positive and negative controls, respectively. As shown in Fig. 7, all strains developed in the presence of 0.1 mM H_2O_2, observing a better development of the triple mutant strain complemented with the coding genes for the Msrs (respect to

the no complemented Msr triple mutant strain). Interestingly, when the H_2O_2 concentration was increased (to 1 mM), only the recombinant strain complemented with *Lin*MsrA1 or *Lin*MsrA2 was able to grow markedly better than the triple mutant (although to a lesser extent than the positive control). Besides, under HClO stress conditions, only *Lin*MsrA1 complemented cells were able to grow and cope even better with stress than the parental strain. These results suggest that the proteins could exhibit different levels of enzymatic activity in the yeast system (being accentuated under oxidative stress conditions) and that *Lin*MsrA1 could have primary antioxidant functions *in vivo*.

3.3 *Kinetic characterization of* Lin*MsrA1,* Lin*MsrA2 and* Lin*MsrB*

As mentioned in the introduction, low molecular mass thiols (such as GSH coupled to Grx), or redox proteins (such as Trx) has been identified as the natural reducing substrates of MsrA or MsrB [55]. Previously, we reported the existence of a functional Trx system in *Leptospira* spp [6]. To quantify the biological function of *Lin*Msrs, we performed enzymatic activity assays using coupled redox systems to evidence the L-MetSO reduction through monitoring the NADPH oxidation at 340 nm. We evaluated the Trx system as a coupled redox cascade consisting of the following steps: (i) NADPH-dependent reduction of TrxR, (ii) reduction of Trx by reduced TrxR, (iii) reduction of Msr by reduced Trx [$Trx(SH)_2$], and (iv) reduction of L-MetSO (or N-AcMetSO) by Msrs. Under these reaction conditions, both *Lin*MsrA1 and *Lin*MsrA2 were functional, indicating that both *Lin*MsrA could employ the Trx system as a physiological reductant (Supplementary data - Fig. 4 and Supplementary data - Fig. 5). *Lin*MsrAs exhibited similar apparent Michaelis-Menten kinetics for *Lin*Trx and the sulfoxide substrates. Both *Lin*MsrA1 and *Lin*MsrA2 were two-order of magnitude more efficient in the reduction of *Lin*Trx than in sulfoxide substrate reduction. The kinetic parameters detailed in Table 2 point out that *Lin*MsrA1C25S and *Lin*MsrA2C18S exhibited lower enzymatic activity than the wild type versions. Particularly, *Lin*MsrA1C25S exhibited between 7 to 18-fold less sulfoxide reduction efficiency than *Lin*MsrA1. Besides, the mutant protein presented between 100 to 160-fold less efficient for Trx oxidation than the wild-type enzyme (Table 2 and Supplementary data - Fig. 4). Under our experimental conditions, the enzymatic activity of *Lin*MsrA2C18S was only detected at high substrate concentrations, which made it difficult to perform its kinetic characterization. Nevertheless, the *Lin*MsrA mutant versions exhibited the

ability to reduce L-MetSO using DTT as a reducer (assayed by TLC assay, Supplementary data - Fig. 6). These results indicated that the mutant proteins are active and suggest that I) the Trx could directly reduce the sulfenic acid intermediate (with much less efficiency) in the oxidized form of *Lin*MsrA1C25S and the *Lin*MsrA2C18S proteins and II) the disulfide bond formation between Cys^{25} and Cys^{165} (for wild-type *Lin*MsrA1) or Cys^{18} and Cys^{175} (for wild-type *Lin*MsrA2) is critical for enzyme reduction by Trx and the concomitant catalytic recycling.

Given the amino acid sequence analyses (above) that suggest that the *Lin*MsrB (the mature form of the protein) is a functional 1-Cys MsrB-type enzyme (lacking resolving Cys residues and exhibiting a stable R-SOH intermediate), we evaluated, in a first approach, an alternative reducing substrate for its catalytic reduction. It has been reported that thio-nitro benzoate (TNB) can act as a non-physiological reductant, allowing the reduction of RSOH intermediate formed after catalytic-thiol oxidation of different proteins, such as *Mycobacterium tuberculosis* AhpE [42, 48]. Therefore, we employed TNB as an alternative substrate for *Lin*MsrB-SOH reduction (the sulfenic protein formed after reaction with sulfoxide substrate). The estimated second-order kinetic constants indicate that the step of formation of the mixed disulfide between MsrB-SOH and TNB is faster ($k´$ = 2167 M^{-1} s^{-1}) than that corresponding to the reduction of the MsrB-SS-TNB mixed disulfide (generated for the action of a second TNB molecule) to produce MsrB-SH (the thiol form) and DTNB ($k´$ = 48 M^{-1} s^{-1}) (see Supplementary data - Fig. 7). Under these reaction conditions, low turnover was observed. These results suggest that a catalyst is required to accelerate the mixed disulfide reduction.

Likely to both *Lin*MsrA proteins, we evaluated if the *Lin*Trx (plus *Lin*TrxR) can reduce *Lin*MsrB in a steady-state kinetics approach. As shown in Supplementary data - Fig. 8, *Lin*MsrB was active with this redox system. However, the calculated catalytic efficiency for *Lin*MsrB reduction by *Lin*Trx is lower (~260-fold) than that the calculated values for both *Lin*MsrAs with the same reducing substrate (Table 2). The kinetics data suggest that the *Lin*Trx is a reducing substrate that could directly reduce the sulfenic acid intermediate of *Lin*MsrB and regenerate the reducing form of the enzyme (similar to *Lin*MsrA mutant proteins). The ability of Trx (or Trx-like proteins) to reduce 1-Cys MsrB was previously described for other enzymes from other organisms [25, 56-58]. As an alternative to the ability of Trx to be reducing substrates, there is evidence that both 1-Cys MsrA as 1-Cys MsrB is efficiently reduced by Grx (plus GSH) [25, 59].

Accordingly, we evaluated as the possible reductant of *Lin*MsrB (in its different metal-variants), a heterologous GSH/Grx system. The GSH regeneration was maintained at the expense of the function of *S. cerevisiae* glutathione reductase in the NADPH-dependent reaction. As shown in Supplementary data - Fig. 9, *Lin*MsrB was active with this redox system. It is noteworthy that the *Lin*MsrB reduction by *Hsa*Grx is 30-fold more efficient than the reduction by *Lin*Trx (Table 2). These results suggest that Grx (together with GSH) is more efficient than Trx in the reduction of the sulfenic acid intermediate present in the catalytic cycle of the *Lin*MsrB. Besides, the calculated kinetics parameters (Table 2) for the reduction of sulfoxide substrate by *Lin*MsrB showed that the enzyme has more affinity and reduction-efficiency for N-AcMet(*R*)SO than L-Met(*R*)SO. Curiously, the values of catalytic efficiencies for sulfoxide reduction by *Lin*MsrB are lower than that calculated for both *Lin*MsrAs by the same substrates (Table 2). These results are in agreement with previous reports of MsrBs from *S. cerevisiae*, *N. meningitidis*, and *E. coli* [12, 60].

To evaluate the ability of *Lin*MsrAs and *Lin*MsrB to reduce oxidized proteins, we assessed the Msr activity of the recombinant enzymes. The assays were performed in the presence of Trx or Grx/GSH as reducing substrate, and a protein extract from *L. interrogans* treated with HClO (which reacts rapidly with Met, [32]) as the sulfoxide substrate. As reference control, we used a protein extract from untreated bacteria. As shown in Fig. 8, Msr activity was only observed with the use of the extract of HClO-treated bacteria (the reaction rate was proportional to the *Lin*Msr concentration). Worthy to note is that *Lin*MsrA1 ($k_{cat\ app}$ = 1.2 ± 0.2 min^{-1}) and *Lin*MsrA2 ($k_{cat\ app}$ = 0.9 ± 0.2 min^{-1}) exhibited similar reductase activity, but higher than *Lin*MsrB ($k_{cat\ app}$ = 0.06 ± 0.01 min^{-1}), similarly to that observed for the free L-MetSO substrate or N-AcMetSO. This result supports that *Lin*Msrs can effectively act on substrates of higher molecular mass, reducing sulfoxide present in proteins.

3.4 *Structural and physical properties of* Lin*Msrs*

To determine the structural and physical properties of the purified recombinant *Lin*Msr proteins, we performed chromatography on Superdex 200 and non-reducing SDS-PAGE studies. *Lin*MsrB eluted from gel filtration as a monomeric protein with a Mr of 18 kDa, while *Lin*MsrA1 and *Lin*MsrA2 eluted as dimeric proteins with Mr of 38 kDa and 40 kDa, respectively (Supplementary data - Fig. 10).

As previously described [46, 61], MsrAs can change their electrophoretic profile in non-reducing SDS-PAGE after incubation of the enzyme with DTT (as reducing agent), or sulfoxide substrate (or other physiological oxidant agents). The highest electrophoretic mobility of L-MetSO-oxidized proteins (compared to full-reduced proteins with DTT) could indicate the formation of an intramolecular disulfide bond between distal Cys residues [62, 63]. Thus, a disulfide bond between distal Cys (in primary structure) residues induces the formation of a more compact structure of the protein (modifying the Stokes radius) and finally changing the electrophoretic motility. As shown in Fig. 9, *Lin*MsrB did not show changes in the non-reducing SDS-PAGE migration (Fig. 9) after treatment with L-MetSO or DTT, suggesting that *Lin*MsrB is a functional 1-Cys MsrB, in agreement with its primary sequence (where no recycling Cys residue is identified). In contrast, the oxidized *Lin*MsrA1 and *Lin*MsrA2 proteins showed bands with greater electrophoretic mobility (compared with the reduced form) after the incubation with L-MetSO. However, when we mutated the vicinal Cys to the nucleophilic Cys (in *Lin*MsrA1C25S or *Lin*MsrA2C18S), the greater electrophoretic migration of protein in the presence of L-MetSO was not observed. This behavior suggests the formation of a disulfide bond between the vicinal Cys residue in the redox-active motif GCFWC (the non-conserved Cys residue present in the active site of MsrAs) and the distal Cys in the primary sequence (the Cys in the C-terminal) after reaction with L-MetSO in wild-type enzymes.

To complement the performed analyzes, we determinate the presence of thiol (R-SH) and sulfenic acid (R-SOH) groups in *Lin*MsrAs before and after reacting with their sulfoxide substrate. As shown in Table 3, after the reduction of proteins with DTT, the detected number of Cys residues in the R-SH form was similar to the total Cys number derivative from amino acid sequences of *Lin*MsrAs (five Cys residues for *Lin*MsrA1, four for *Lin*MsrA1C25S, three Cys for *Lin*MsrA2 and two for *Lin*MsrA2C18S). After the reaction of the R-SH form of *Lin*MsrAs with L-MetSO (at 1:50 molar ratio), we detected three remaining R-SH groups for *Lin*MsrA1 and *Lin*MsrA1C25S; and one remaining R-SH group for *Lin*MsrA2 and *Lin*MsrA2C18S. Besides, we could not detect post-reaction stable R-SOH groups for *Lin*MsrA1 or *Lin*MsrA2. However, for *Lin*MsrA1C25S and *Lin*MsrA2C18S, one Cys residue (approximately) in the R-SOH form was detected in each mutant protein. Worthy of note is that the difference in R-SH group number between reduced and oxidized forms of *Lin*MsrA1 or *Lin*MsrA2 indicates the consumption of two R-SH groups, suggesting a possible thiol-disulfide exchange

reaction mechanism. In line with the above, the difference in R-SH group number between reduced and oxidized forms of *Lin*MsrA1C25S or *Lin*MsrA2C18S indicates the consumption of one R-SH group with the concomitant formation of an R-SOH group in each mutant protein. The obtained results of thiol and sulfenic acid titration suggest that the vicinal Cys residue in the redox-active motif GCFWC of *Lin*MsrA1 (Cys^{25}) and *Lin*MsrA2 (Cys^{18}) participate in the catalytic mechanism (as resolutive Cys intermediary) together to the conserved catalytic Cys present in the redox-active motif. Our data indicated that the vicinal Cys residue in the GCFWC active motif is critical for the regeneration of the nucleophilic Cys to R-SH form after the L-MetSO reduction step. This conjecture is based on the observation that the *Lin*MsrA mutant versions of Cys^{25} of *Lin*MsrA1 and Cys^{18} of *Lin*MsrA2 present stable R-SOH after MetSO reduction. Thus, the vicinal Cys of the redox-active site (after the resolution of R-SOH form of nucleophilic Cys in active-redox site) and C-terminal Cys residue would operate in the formation and isomerization of the intermediate disulfide bond, which would be reducible by Trx. Interestingly, at a higher MsrA:MetSO molar ratio (1:500), one more thiol group was consumed (with the concomitant detection of one sulfenic group) in both *Lin*MsrA wild-type proteins. We hypothesize that second oxidation of the resolutive Cys thiol (post-isomerization of a first resolutive disulfide in the active site) would occur more slowly (and therefore detectable at higher MsrA:MetSO molar ratio) due to the existence of a steric impediment to the binding of the sulfoxide substrate in the active site by the presence of the disulfide formed in the environment of the active site (between the extra Cys of the active site motif and the Cys C-terminal).

The proposal for a catalytic mechanism of MsrAs is via a Cys triad (with a resolutive disulfide isomerization) is supported by the results of non-reducing SDS-PAGE assays, where, the wild-type variants exhibited an electrophoretic mobility gain after MetSO treatment (in contrast to the *Lin*MsrA1C25S and *Lin*MsrA2C18S proteins that lack this electrophoretic mobility gain after reaction with MetSO). This highest electrophoretic mobility of L-MetSO-oxidized proteins suggests the formation of an intramolecular disulfide bond between distal Cys residues (in primary structure, as was described for other MsrA proteins [46]). Complementary, we performed molecular modeling of the *Lin*Msr proteins. The building of the structural models was based on templates detailed in the Material and Methods section, derived from the known X-ray structure of the homologous enzymes. Fig. 10 A-B depicts the models for *Lin*MsrA1 and *Lin*MsrA2, highlighting the putative Cys triad involved in the catalytic mechanism of these

proteins. In the case of *Lin*MsrA1, the shown residues are the Cys^{22}, Cys^{25} (from the CFWC catalytic motif), and the Cys^{165} (which could act as second resolving Cys). Based on our three-dimensional model, the Cys^{165} locates at a close distance (15 Å) from Cys^{25}. For *Lin*MsrA2, the highlighted residues are Cys^{15}, Cys^{18} (from the CFWC catalytic motif), and the Cys^{175} (which could act as the second resolving Cys since it is to ~5 Å distance from Cys^{18}). The generation of *Lin*MsrA1C25S and *Lin*MsrA2C18S mutants supports the role of the extra Cys residues in the catalytic mechanism. This mechanism has been demonstrated for 3-Cys MsrAs from other organisms [11, 17, 55].

For *Lin*MsrB, after the DTT treatment, only one of the five theoretical Cys residues was identified as an R-SH group (Table 3). The latter indicates that the other four Cys residues of *Lin*MsrB (which could be involved in the binding of the metal atom) did not react with DTNB and, therefore, could not be detected. One Cys residue in the R-SOH form was detected in the protein after L-MetSO incubation. This R-SOH group is detectable since it is more stable due to the absence of a resolving Cys in *Lin*MsrB. These results reinforce that only one Cys is involved in the reaction with L-MetSO, allowing us to classify *Lin*MsrB as a functional 1-Cys MsrB, following its primary sequence. As was noted in the sequence alignment (Fig. 3), MsrB proteins present four Cys residues constituting a metal-binding site (specifically Zn) [11]. Given this, recombinant *Lin*MsrB produced from *E. coli* BL21 (DE3) cultures in LB medium was analyzed by flame spectrophotometry. The obtained results indicate that the protein thus generated has a 30% of metal atom occupancy, being mostly Zn and, to a lesser extent, Fe (91 and 9%, respectively). To obtain homogenous populations of the recombinant protein in the presence (and absence) of a particular metal atom, we produced the protein using an M9 medium supplemented with $ZnCl_2$, $FeCl_2$, or $CoCl_2$, purified by IMAC and analyzed again by flame spectrophotometry. All the different metal-bound versions of *Lin*MsrB were obtained with a high degree of purity and presented metal atom occupancy between 30 to 40% (Supplementary data - Fig. 11). Besides, the *Lin*MsrB isoforms that bind Co and Fe exhibit the characteristic absorption peaks in the UV-Visible spectrum (Supplementary data - Fig. 11). Fe-*Lin*MsrB shows an absorption peak at 350 nm, while Co-*Lin*MsrB shows two absorption peaks at 372 nm and 485 nm (Supplementary data - Fig. 11). Interestingly, the addition of EDTA (at 1:1000 protein mol:EDTA mol) did not modify the spectroscopic profiles of both isoforms (Fe-*Lin*MsrB and Co-*Lin*MsrB, data not shown), suggesting that the protein has a high affinity for the metal atom, as was reported for the Se-MsrB of *Drosophila*

melanogaster [64]. Besides, different *Lin*MsrB metal variants showed identical catalytic efficiencies regarding L-Met(*R*)SO reduction (Supplementary data - Fig. 11). However, metal-free *Lin*MsrB showed ~1% of catalysis efficiencies for sulfoxide reduction comparing with metal-bound variants for sulfoxide reduction (Supplementary data - Fig. 11). Similar to spectroscopy assays, the addition of EDTA (up to 1:100000 mol protein: mol EDTA) did not modify the enzymatic activity of the metal-bound enzymes (data not shown). These results indicate, *a priori*, that the presence, but not the nature, of the metal atom, would be necessary for sulfoxide reductase activity. Similar results were previously presented for the mammalian MsrB [28]. Fig. 10C exhibits the molecular model obtained for *Lin*MrsB, where the residues Cys^{48}, Cys^{51}, Cys^{97}, and Cys^{111} form the structural $Zn(Cys)_4$ complex. Besides, we also highlighted the residue Cys^{120}, which is the putative essential catalytic residue located in a conserved motif (R(Y/H)C(I/V) at the C-terminal, which forms a β-sheet.

3.5. *Msrs activity is present in* L. interrogans *cells*

To determine the presence of Msr proteins in *L. interrogans* cells, we performed western blot assays of the soluble and membrane-associated fractions from a pool of three bacterial cultures. In such a study, we used polyclonal antibodies against *Lin*MsrAs and *Lin*MsrB and, as detection controls, against a soluble cytoplasmatic (*Lin*TrxR) as well as a transmembrane (Lp32) protein. As illustrated in Fig. 11, *Lin*MsrB was detected in the soluble fraction, while a signal in both soluble (mainly) and the membrane-associated fraction was observed for *Lin*MsrA. The serum used exhibited cross-reactivity for both *Lin*MsrA1 and *Lin*MsrA2 (data not shown), which did not distinguish the specific isoform detected. The SOSUI and SignalP predictors suggest that *Lin*MsrA1 is a soluble protein, whereas $LinMsrA2_{SP}$ is a protein harboring a hydrophobic N-terminal signal peptide to the periplasm, which could explain why MsrA proteins are detected in both fractions. According to *in silico* predictions, $LinMsrA2_{SP}$ and $LinMsrB_{SP}$ have a putative N-terminal extension that could be a transit peptide towards the periplasmic space in *L. interrogans*. Because of this, we performed a digitonin cellular fractionation of *L. interrogans* cells to obtain a cytoplasmic (identified with antibodies against *Lin*TrxR and *Lin*AhpC) and a periplasmic (detected with anti-*Lin*catalase [4]) enriched fractions. Fig. 12 shows that *Lin*MsrAs and *Lin*MsrB were detected in all fractions (both periplasmic and

cytoplasmic fractions). These results suggest that *Lin*Msrs have both periplasmic and cytoplasmic localization in the bacteria.

Besides, we assayed the enzymatic activity in soluble crude extracts of exponential phase growing *L. interrogans*, taking into account the substrate specificity of each type of Msr detailed in Table 2. Msr activity was evaluated following the oxidation of NADPH at 340 nm at 30 °C and pH 7.0, and also using different quantities of cell proteins soluble extract. For this determination, we used the MetSO isomers (*S* or *R*) separately with the *L. interrogans* Trx system or the heterologous GSH/Grx as the electron donor. In this way, a MsrA specific enzymatic activity of 21 ± 6 mU mg^{-1} was detected using L-Met(*S*)SO, and the *L. interrogans* Trx system as substrates. Furthermore, when the *R* isomer replaced the *S* isomer in the same reaction conditions, Msr activity was only evident with the heterologous GSH/Grx system. The MsrB specific enzymatic activity detected in this condition was 5 ± 1 mU mg^{-1}, in agreement with the observed recombinant *Lin*MsrB functional characteristics. As a whole, these results indicate the occurrence of Msr activity in *L. interrogans* cells.

3.6. *Reversion of* Lin*catalase inactivation caused by HClO*

The *Lin*catalase could be inactivated by HClO in a DTT-insensitive manner, which is compatible with structural changes in the protein related to the oxidation of Met residues (Fig. 13), similarly to a previous report for the enzyme *Helicobacter pylori* [65-67]. After this, the question arose if *Lin*Msrs could reverse such HClO-dependent inactivation of *Lin*catalase. To test for an answer, we performed an *in vitro* assay where *Lin*catalase partially inactivated by HClO was incubated in the presence of different reductants, including *Lin*MsrB or *Lin*MsrAs. As shown in Fig. 13, the *Lin*catalase activity was recovered by ~25% in the presence of *Lin*MsrB. This result supports the view that part of the enzyme inactivation caused by HClO would be due to Met oxidation with the formation of the Met(*R*)SO isomer. However, the low recovery of catalase functionality mediated by *Lin*MsrB would require chaperone-type proteins, which help in the process of functional folding. This synergistic action of MsrB and chaperone in the recuperation of activity was previously reported for the *H. pylori* catalase [65-67]. Since MsrB and catalase were detected in the same cellular fraction in *L. interrogans*, it is tempting to speculate that both proteins interact in a physiological context in the bacteria.

4. DISCUSSION AND CONCLUSIONS

L. interrogans is the causative agent of leptospirosis, a disease with a mortality of about 30%. In humans, the infection severity varies with the serovar of Leptospira involved and its virulence, together with the health and immune status of the patient. Pathogenic leptospiras are invasive, mainly due to their ability to survive and grow in tissues, escaping natural host-defense mechanisms, such as complement system and phagocytic cells, similar to other microbial pathogens [2, 68, 69]. *L. interrogans* genome project offers information of nucleotide sequences coding for two MsrAs and one MsrB. Therefore, we present here a functional characterization of three Msrs from the etiologic agent of Leptospirosis disease. We evidenced that similar to Msrs from other organisms [70], *Lin*MsrAs and *Lin*MsrB are not homologous proteins. This diversity in the primary structure confers differences in the tridimensional structure and substrate specificities, although they catalyze the same chemical reaction and share similar primary reaction mechanism. Our results aim to contribute to the right assignment of structure-function relationships for these enzymes, adding value to the data available from the genome project of this bacterium.

In a first approach, we evaluated their functionality *in vivo* performing complementation assays of an Msr mutant yeast strain (lacking the three types of endogenous Msrs). The recombinant yeasts supplemented with the genes coding for *Lin*Msrs were able to develop in the presence of L-MetSO, indicating that the three proteins were functional *in vivo*. By using TLC assays, we confirmed the *in vitro* activity and the isomer specificity of the three proteins (using DTT as reducing substrate). Besides, by *in vitro* coupled assays (using the recombinant enzymes), we evaluated the ability of *Lin*Msrs to reduce oxidized proteins from *L. interrogans*. The results indicate that *Lin*Msrs can effectively act on substrates of higher molecular mass, reducing sulfoxide present in proteins. These approaches allow us to conclude that proteins are functional to continue with their characterization.

The amino acid sequences of *Lin*MsrA1 and *Lin*MsrA2 exhibit similar identity to other MsrA enzymes from other organisms. A noteworthy feature is that in both *L. interrogans* MsrAs present an extra Cys residue in the conserved redox-active motif of MsrA enzymes (GCFWC in the redox-active site of *Lin*MsrAs). Experimentally, until now, this unusual structural characteristic was observed in the MsrA enzyme from *B. subtilis* [11]. The presence of this vicinal Cys residue in the active site of *Lin*MsrAs, allows us to hypothesize that this residue is a putative resolutive Cys (the

catalytic and a possible resolutive Cys are vicinal residues). To evaluate this hypothesis, we generated mutant variants of these proteins in this extra Cys residue in the active site and we continued their comparative study concerning the wild-type proteins.

The kinetic characterization of wild-type *Lin*MsrAs showed that they have similar catalytic efficiencies when using L-Met(*S*)SO and N-AcMet(*S*)SO as substrates. Similar values of catalytic efficiencies have been described for Msrs purified from *E. coli*, *N. meningitidis*, and *P. trichocarpa* [11, 71, 72]. Our experimental data exhibited that oxidized *Lin*MsrAs was reduced by *Lin*Trx, a common reducing agent for most described MsrAs [11, 27, 73]. In the catalytic cycle of MsrAs, the efficiency for L-Met(*S*)SO [or N-AcMet(*S*)SO] reduction is lower than the efficiency for *Lin*Trx oxidation (suggest that the rate-limiting step in the MsrAs catalytic cycle is the sulfoxide reduction). Other authors reported similar behavior in *E. coli* MsrA [71]. Interestingly, the MsrA-reduction by Trx step is less catalytically efficient for *Lin*MsrA1C25S or *Lin*MsrA2C18S than for wild-type isoforms. These results added to the thiol/sulfenic acid titration assays, non-reducing SDS-PAGE experiments, and molecular modeling suggest that both *Lin*MsrAs follow a Cys-triad catalytic mechanism (by the formation and isomerization of the intermediate disulfide bond) mediated via the extra Cys residue present in the redox-active site (GCFWC). The proposed mechanism is that the nucleophilic Cys, present in the GCFWC motif, react with the sulfoxide substrate, forming the R-SOH intermediate. Then, the second Cys in the GCFWC motif attacks the R-SOH intermediate with the consequent formation of an intramolecular disulfide bond (between the vicinal Cys residues). The isomerization of such intermediate disulfide would involve a third Cys, located at the C-terminus of *Lin*MsrAs (spatially close to the GCFWC motif in the tridimensional model). Finally, the isomerized disulfide bond is efficiently reduced by Trx to complete the catalytic cycle. The idea of a formation of an intermediate disulfide that isomerizes to a more "reactive" disulfide bond is consistent with the observations that the mutant versions of MsrAs: 1) are less efficiently reduced by Trx (without losing the ability to reduce a sulfoxide substrate efficiently, similar to the wild-type versions); 2) exhibit the presence of intermediate sulfenic acid after MetSO reaction at low MsrA:MetSO molar ratio (unlike to wild-type versions, where this functional group is not detected despite the consumption of thiol groups after reaction with MetSO); and 3) lack the increase in the electrophoretic mobility in non-reducing SDS-PAGE experiments after

MetSO reduction (in contrast to wild-type versions, where is observed an increase in the electrophoretic mobility of L-MetSO-oxidized proteins, regarding full reduced proteins with DTT, by the presence of an intramolecular disulfide bond between spatially distal Cys residues). Added to the above, the detection of a MetSO-dependent second oxidation event (one more thiol group is consumed with the concomitant detection of one sulfenic group) in wild-type MsrA proteins (in this case at a high MsrA:MetSO molar ratio) is consistent with a catalytic mechanism that comprises a Cys triad (in 3-Cys Msrs, with isomerization of disulfide bonds), as previously observed for other Msrs (both type A and B [74 81, 75 85]). We hypothesize that second oxidation of the resolutive Cys thiol (post-isomerization of a first resolutive disulfide in the active site) would occur more slowly (and therefore detectable at higher MsrA:MetSO molar ratio) because due to the existence of a steric impediment to the binding of the sulfoxide substrate in the active site by the presence of the disulfide formed in the environment of the active site (between the extra Cys of the active site motif and the Cys C-terminal). One interesting aspect of our observations on the catalytic mechanism proposed for *Lin*MsrAs is that the "pivot" Cys residue (in the formation of the isomerized disulfide bond) is present in the redox-active motif of enzymes (as vicinal residue to nucleophilic Cys residue). The proposed catalytic mechanism is schematized in Fig. 14. To our knowledge, it is the first functional description of MsrA enzymes with a vicinal resolutive Cys residue in the active site.

The amino acid sequence of *Lin*MsrB exhibits a SelB structural folding, which is a characteristic in MsrB proteins [70]. Such a domain presents two CXXC motifs that conform to the metal-binding site (with Zn mainly) [55, 76]. In *Lin*MsrB, we identified (by sequence identity) four Cys residues (Cys^{48}, Cys^{51}, Cys^{97}, and Cys^{111}) involved in the binding of the Zn atom. Additionally, we identified one conserved Cys residue (Cys^{120}) responsible for L-Met(*R*)SO reduction. Similar to other MsrB proteins lacking a resolving Cys [11], the formation of a stable R-SOH intermediate in their catalytic cycle was detected, and the recycle (its reduction to R-SH) was dependent on low-molecular-mass thiols (such as GSH). Complementarily, regarding the CXXC motif, it was possible to cluster MsrBs of pathogenic and free-living *Leptospira* species phylogenetically. The clade where *Lin*MsrB clustered, possesses a consensus sequence CA(G/A)C, which was different from the group where is *L. biflexa* MsrB, which contains a CVCC motif.

According to thiol/sulfenic acid titration, and kinetics properties, *Lin*MsrB is a 1-Cys MsrB (without resolving Cys). During the catalytic cycle, the formation of a stable R-SOH was observed through titration with NBD-HCl and assays with TNB. In the latter, the recycling of this stable intermediate is the limiting step during the regeneration (reduction) process of mixed disulfide intermediary (TNB-S-S-MsrB). This behavior is similar to the reported for TNB-dependent reduction (to thiol) of other sulfenic acid proteins [42, 48]. Steady-state kinetics experiments indicated that the catalytic recycle of oxidized *Lin*MsrB (the sulfenic acid intermediate reduction in the enzyme) was performed more efficiently by the action of the GSH/Grx system than the Trx system (unlike to *Lin*MsrA proteins). A proposed generic catalytic mechanism for *Lin*MsrB is schematized in Fig. 14. The specificity of *Lin*MsrB by the GSH/Grx redox pair represents a starting point to deepen the study of the endogenous Grx occurrence in this bacterium. It is noteworthy that we have recently described the presence of active GSH-dependent metabolism in this bacterium [77]. Our results hypothetically interconnect both Trx and Grx in the recycling of different types of Msrs, whose joint action would be necessary for reverse the oxidation of Met residues.

As we evidenced in the results section, *Lin*MsrB is a metalloprotein, and its metal variants exhibited similar catalytic efficiencies. A comparable behavior was informed for the mammalian MsrB1, where the substitution of Zn by Co generated a protein with similar levels of Msr activity [28]. In contrast, the free-metal enzyme presented a lower efficiency of catalysis for L-MetSO reduction than isoforms with metal atoms. Therefore, it was proposed that the presence of the metal could contribute to the correct folding of the protein. Besides, *Lin*MsrB was able to reduce both, free L-Met(*R*)SO and N-AcMet(*R*)SO, but their catalytic efficiencies were lower than those obtained with *Lin*MsrAs, consistent with previous reports [60]. Given the lack of identification of a sequence coding for a free Msr-like protein (MsrC), the ability of *Lin*MsrB to reduce L-Met(*R*)SO could have significant importance for the bacteria. Several MsrC (or *f*Msr) proteins were detected in unicellular organisms like bacteria and yeasts [60]. They have high specificity for the *R* isomer of free L-MetSO, compensating the low activity showed by MsrBs and allowing, in consequence, efficient recovery of free L-Met oxidized [50, 60].

The fractionation assay results suggest that *Lin*Msrs have both periplasmic and cytoplasmic localization in *L. interrogans*. This is an interesting behavior because it offers the possibility of exhibiting the ability to reduce MetSO-proteins in both

compartments and thus contribute to redox homeostasis. This thiol-dependent Msr activity dual localization was observed in other pathogenic bacteria such as *Streptococcus pneumoniae* [78], *Streptococcus gordonii* [79], *Staphylococcus aureus* [80], and *Neisseria meningitidis* [81]. In view that the *L. interrogans* canonical Trx system (as well as a putative Grx and the GSH) exhibits a cytoplasmic location, a question to be asked is, what other system or redox protein could be a substrate for the Msrs in the periplasm? Attending to a possible answer to this question, by analyzing the *L. interrogans* genomic information, we found coding sequences for a putative periplasmic Trx-like protein (LIC10278), a thiol:disulfide interchange protein (DsbA, LIC11629), and a disulfide interchange transmembrane protein (DsbD, LIC12404). These thiol-dependent redox proteins could be a source of reducing equivalents and catalyze the reduction of the intermediate disulfide in the case of *Lin*MsrAs or the intermediate sulfenic acid in *Lin*MsrB (see Fig. 14), thus regenerating the Msrs to their (reduced) thiol form in the periplasm of *L. interrogans* (as already described for other bacteria [9, 81]). This hypothesis tempts us to propose new experiments that will be evaluated in future studies.

Previous works reported that in *L. interrogans*, catalase is an abundant protein and a virulence factor, given that it is the main responsible for bacterial viability under H_2O_2 exposition [4, 82, 83]. *Lin*catalase is a Met rich protein, and HClO has high reactivity towards such residues [67]. HClO-mediated Met oxidation can lead to forming $MetSO_2$ (Met-sulfone), an irreversible modification that might generate protein misfolding and aggregation [67]. In consequence, this type of stress conduces to the expression of proteases and chaperones, and in extreme conditions, damaged proteins are degraded [84]. Particularly, the loss of function of *Lin*catalase at the expense of HClO was related to changes in its structure (inducing the formation of oligomers of higher molecular mass, data unpublished). Interestingly, our results suggest that *Lin*MsrB could partially reverse the HClO-dependent inactivation of *Lin*catalase. This latter means, on the one hand, that *Lin*MsrB can regenerate Met oxidized in proteins. The partial recovery of catalase activity could be linked to the requirement of a combined action between Msr and chaperones, as described for the enzyme from *H. pylori* [65-67]. Combining the *in vitro* assays of the recovery of catalase activity (inactivated by HClO mediated by MsrB) with the periplasmic localization observed for both proteins, we speculate that these proteins are a redox partner *in vivo*. The maintenance of functional *Lin*catalase

could be essential for bacterial survival in the presence of oxidative stress. Therefore, both MsrB and catalase could be related to bacteria pathogenicity and virulence.

Using genomic data, we could identify one member of Msr-like proteins in *L. interrogans*, a molybdenum-dependent biotin sulfoxide reductase enzyme, bisC (LIC10874). The primary function of biotin sulfoxide reductase is to mitigate the effects of oxidative damage to biotin [9]. However, recent work on *E.coli* and *Salmonella typhimurium* has uncovered that the bisC likely has a second function in L-MetSO reduction [9]. Besides, no encoding sequences are reported in *L. interrogans* genome project for methionine sulfoxide reductase P (MsrP, a periplasmic molybdenum-dependent enzyme) or dimethyl sulfoxide reductase (DmsA). These enzymes are present in other bacteria (such as *E. coli* [85, 86] and *S. typhimurium* [87]) and have been shown to reduce MetSO [9]. *In silico* analysis suggest that the amino acid sequence of *L. interrogans* BisC protein would not present signaling peptide or transmembrane domains, indicating that this protein is a possible cytoplasmic enzyme. The latter, added to the possible absence of MsrP and DmsA homologous, gives value to the detection of *Lin*MsrA and *Lin*MsrB in the periplasm of *L. interrogans* as potential thiol-dependent antioxidant enzymes for repairing oxidized proteins. The latter is similar to that reported for *S. pneumoniae [78], S. gordonii* [79], *S. aureus* [80], and *N. meningitidis* [81].

As a whole, the results herein contribute to the understanding of the redox metabolism present in *L. interrogans*, to the establishment of structure/function relationship and determination of possible interaction among the enzymes involved in it. Besides, our results constitute the starting point to evaluate further the regulation mechanisms of those enzymes, which are part of antioxidant systems, as well as to decipher their possible implication in the virulence and pathogenicity for the bacteria under study.

ACKNOWLEDGMENTS

We thank Dr. Vadim N. Gladyshev (Department of Medicine, Brigham and Women's Hospital, Harvard Medical School, Boston, MA, USA) for *Saccharomyces cerevisiae* GY202 cells. This work was supported by grants from ANPCyT (PICT2014-2103, PICT2016-1778, and PICT2017-2268) and Fundación Bunge y Born (Subsidios Fundación Bunge y Born para investigación de la enfermedad de Chagas – 2016). N.S. is a fellow from ANPCyT (Argentina). AAI, SAG, and DGA are investigator career members from CONICET.

CRediT author statement:

Natalia Sasoni: Conceptualization, Methodology, Validation, Formal analysis, Investigation, Writing - Original Draft, Visualization.

Matías D. Hartman: Software, Visualization, Review & Editing.

Sergio A. Guerrero: Conceptualization, Writing - Review & Editing, Funding acquisition, Resources.

Alberto A. Iglesias: Conceptualization, Writing - Review & Editing, Funding acquisition, Resources.

Diego G. Arias: Conceptualization, Methodology, Validation, Formal analysis, Investigation, Supervision, Visualization, Writing - Review & Editing, Project administration, Resources, Funding acquisition.

Declaration of interests

☒ The authors declare that they have no known competing financial interests or personal relationships that could have appeared to influence the work reported in this paper.

REFERENCES

[1] R.E. Morey, R.L. Galloway, S.J. Bragg, A.G. Steigerwalt, L.W. Mayer, P.N. Levett, Species-specific identification of Leptospiraceae by 16S rRNA gene sequencing, J Clin Microbiol, 44 (2006) 3510-3516.

[2] S.X. Ren, G. Fu, X.G. Jiang, R. Zeng, Y.G. Miao, H. Xu, Y.X. Zhang, H. Xiong, G. Lu, L.F. Lu, H.Q. Jiang, J. Jia, Y.F. Tu, J.X. Jiang, W.Y. Gu, Y.Q. Zhang, Z. Cai, H.H. Sheng, H.F. Yin, Y. Zhang, G.F. Zhu, M. Wan, H.L. Huang, Z. Qian, S.Y. Wang, W. Ma, Z.J. Yao, Y. Shen, B.Q. Qiang, Q.C. Xia, X.K. Guo, A. Danchin, I. Saint Girons, R.L. Somerville, Y.M. Wen, M.H. Shi, Z. Chen, J.G. Xu, G.P. Zhao, Unique physiological and pathogenic features of Leptospira interrogans revealed by whole-genome sequencing, Nature, 422 (2003) 888-893.

[3] B. Adler, Current Topics in Microbiology and Immunology: Leptospira and Leptospirosis, Springer, Place Published, 2014.

[4] A. Eshghi, K. Lourdault, G.L. Murray, T. Bartpho, R.W. Sermswan, M. Picardeau, B. Adler, B. Snarr, R.L. Zuerner, C.E. Cameron, Leptospira interrogans catalase is required for resistance to H2O2 and for virulence, Infect Immun, 80 (2012) 3892-3899.

[5] D.G. Arias, A. Reinoso, N. Sasoni, M.D. Hartman, A.A. Iglesias, S.A. Guerrero, Kinetic and structural characterization of a typical two-cysteine peroxiredoxin from Leptospira interrogans exhibiting redox sensitivity, Free Radic Biol Med, 77 (2014) 30-40.

[6] N. Sasoni, A.A. Iglesias, S.A. Guerrero, D.G. Arias, Functional thioredoxin reductase from pathogenic and free-living Leptospira spp, Free Radic Biol Med, 97 (2016) 1-13.

[7] D.B. Oien, J. Moskovitz, Substrates of the methionine sulfoxide reductase system and their physiological relevance, Curr Top Dev Biol, 80 (2008) 93-133.
[8] A.V. Peskin, R. Turner, G.J. Maghzal, C.C. Winterbourn, A.J. Kettle, Oxidation of methionine to dehydromethionine by reactive halogen species generated by neutrophils, Biochemistry, 48 (2009) 10175-10182.
[9] U. Kappler, M. Nasreen, A. McEwan, New insights into the molecular physiology of sulfoxide reduction in bacteria, Adv Microb Physiol, 75 (2019) 1-51.
[10] J. Moskovitz, J.M. Poston, B.S. Berlett, N.J. Nosworthy, R. Szczepanowski, E.R. Stadtman, Identification and characterization of a putative active site for peptide methionine sulfoxide reductase (MsrA) and its substrate stereospecificity, J Biol Chem, 275 (2000) 14167-14172.
[11] S. Boschi-Muller, A. Olry, M. Antoine, G. Branlant, The enzymology and biochemistry of methionine sulfoxide reductases, Biochim Biophys Acta, 1703 (2005) 231-238.
[12] A. Drazic, J. Winter, The physiological role of reversible methionine oxidation, Biochim Biophys Acta, 1844 (2014) 1367-1382.
[13] J. Moskovitz, S. Bar-Noy, W.M. Williams, J. Requena, B.S. Berlett, E.R. Stadtman, Methionine sulfoxide reductase (MsrA) is a regulator of antioxidant defense and lifespan in mammals, Proc Natl Acad Sci U S A, 98 (2001) 12920-12925.
[14] J. Moskovitz, E. Flescher, B.S. Berlett, J. Azare, J.M. Poston, E.R. Stadtman, Overexpression of peptide-methionine sulfoxide reductase in Saccharomyces cerevisiae and human T cells provides them with high resistance to oxidative stress, Proc Natl Acad Sci U S A, 95 (1998) 14071-14075.
[15] M.J. Rodrigo, J. Moskovitz, F. Salamini, D. Bartels, Reverse genetic approaches in plants and yeast suggest a role for novel, evolutionarily conserved, selenoprotein-related genes in oxidative stress defense, Mol Genet Genomics, 267 (2002) 613-621.
[16] J. Moskovitz, M.A. Rahman, J. Strassman, S.O. Yancey, S.R. Kushner, N. Brot, H. Weissbach, Escherichia coli peptide methionine sulfoxide reductase gene: regulation of expression and role in protecting against oxidative damage, J Bacteriol, 177 (1995) 502-507.
[17] S. Lourenco Dos Santos, I. Petropoulos, B. Friguet, The Oxidized Protein Repair Enzymes Methionine Sulfoxide Reductases and Their Roles in Protecting against Oxidative Stress, in Ageing and in Regulating Protein Function, Antioxidants (Basel), 7 (2018).
[18] J.A. Maupin-Furlow, Methionine Sulfoxide Reductases of Archaea, Antioxidants (Basel), 7 (2018).
[19] P. Rey, L. Tarrago, Physiological Roles of Plant Methionine Sulfoxide Reductases in Redox Homeostasis and Signaling, Antioxidants (Basel), 7 (2018).
[20] B. Jiang, J. Moskovitz, The Functions of the Mammalian Methionine Sulfoxide Reductase System and Related Diseases, Antioxidants (Basel), 7 (2018).
[21] Z. Lin, L.C. Johnson, H. Weissbach, N. Brot, M.O. Lively, W.T. Lowther, Free methionine-(R)-sulfoxide reductase from Escherichia coli reveals a new GAF domain function, Proc Natl Acad Sci U S A, 104 (2007) 9597-9602.
[22] H.S. Kim, G.H. Kwak, K. Lee, C.H. Jo, K.Y. Hwang, H.Y. Kim, Structural and biochemical analysis of a type II free methionine-R-sulfoxide reductase from Thermoplasma acidophilum, Arch Biochem Biophys, 560 (2014) 10-19.
[23] A. Gruez, M. Libiad, S. Boschi-Muller, G. Branlant, Structural and biochemical characterization of free methionine-R-sulfoxide reductase from Neisseria meningitidis, J Biol Chem, 285 (2010) 25033-25043.

[24] E.H. Lee, G.H. Kwak, M.J. Kim, H.Y. Kim, K.Y. Hwang, Structural analysis of 1-Cys type selenoprotein methionine sulfoxide reductase A, Arch Biochem Biophys, 545 (2014) 1-8.
[25] C. Vieira Dos Santos, E. Laugier, L. Tarrago, V. Massot, E. Issakidis-Bourguet, N. Rouhier, P. Rey, Specificity of thioredoxins and glutaredoxins as electron donors to two distinct classes of Arabidopsis plastidial methionine sulfoxide reductases B, FEBS Lett, 581 (2007) 4371-4376.
[26] H.Y. Kim, Glutaredoxin serves as a reductant for methionine sulfoxide reductases with or without resolving cysteine, Acta Biochim Biophys Sin (Shanghai), 44 (2012) 623-627.
[27] A. Olry, S. Boschi-Muller, H. Yu, D. Burnel, G. Branlant, Insights into the role of the metal binding site in methionine-R-sulfoxide reductases B, Protein Sci, 14 (2005) 2828-2837.
[28] E. Shumilina, O. Dobrovolska, R. Del Conte, H.W. Holen, A. Dikiy, Competitive cobalt for zinc substitution in mammalian methionine sulfoxide reductase B1 overexpressed in E. coli: structural and functional insight, J Biol Inorg Chem, 19 (2014) 85-95.
[29] C. Zhao, A. Hartke, M. La Sorda, B. Posteraro, J.M. Laplace, Y. Auffray, M. Sanguinetti, Role of methionine sulfoxide reductases A and B of Enterococcus faecalis in oxidative stress and virulence, Infect Immun, 78 (2010) 3889-3897.
[30] J.M. Atack, D.J. Kelly, Contribution of the stereospecific methionine sulphoxide reductases MsrA and MsrB to oxidative and nitrosative stress resistance in the food-borne pathogen Campylobacter jejuni, Microbiology, 154 (2008) 2219-2230.
[31] A. Romsang, S. Atichartpongkul, W. Trinachartvanit, P. Vattanaviboon, S. Mongkolsuk, Gene expression and physiological role of Pseudomonas aeruginosa methionine sulfoxide reductases during oxidative stress, J Bacteriol, 195 (2013) 3299-3308.
[32] B. Manta, V.N. Gladyshev, Regulated methionine oxidation by monooxygenases, Free Radic Biol Med, 109 (2017) 141-155.
[33] B.C. Lee, H.M. Lee, S. Kim, A.S. Avanesov, A. Lee, B.H. Chun, G. Vorbruggen, V.N. Gladyshev, Expression of the methionine sulfoxide reductase lost during evolution extends Drosophila lifespan in a methionine-dependent manner, Sci Rep, 8 (2018) 1010.
[34] T.F. Lavine, The formation, resolution, and optical properties of the diastereoisomeric sulfoxides derived from L-methionine, J Biol Chem, 169 (1947) 477-491.
[35] H.C. Ellinghausen, W.G. McCullough, Nutrition of Leptospira Pomona and Growth of 13 Other Serotypes: Fractionation of Oleic Albumin Complex and a Medium of Bovine Albumin and Polysorbate 80, Am J Vet Res, 26 (1965) 45-51.
[36] R.C. Johnson, V.G. Harris, Differentiation of pathogenic and saprophytic letospires. I. Growth at low temperatures, J Bacteriol, 94 (1967) 27-31.
[37] H. Louvel, M. Picardeau, Genetic manipulation of Leptospira biflexa, Curr Protoc Microbiol, Chapter 12 (2007) Unit 12E 14.
[38] J. Sambrook, D.W. Russell, Molecular Cloning: A laboratory manual., Place Published, 2001.
[39] U.K. Laemmli, Cleavage of structural proteins during the assembly of the head of bacteriophage T4, Nature, 227 (1970) 680-685.
[40] M.M. Bradford, A rapid and sensitive method for the quantitation of microgram quantities of protein utilizing the principle of protein-dye binding, Anal Biochem, 72 (1976) 248-254.
[41] G.L. Ellman, Tissue sulfhydryl groups, Arch Biochem Biophys, 82 (1959) 70-77.

[42] L. Turell, H. Botti, S. Carballal, G. Ferrer-Sueta, J.M. Souza, R. Duran, B.A. Freeman, R. Radi, B. Alvarez, Reactivity of sulfenic acid in human serum albumin, Biochemistry, 47 (2008) 358-367.
[43] H.R. Ellis, L.B. Poole, Novel application of 7-chloro-4-nitrobenzo-2-oxa-1,3-diazole to identify cysteine sulfenic acid in the AhpC component of alkyl hydroperoxide reductase, Biochemistry, 36 (1997) 15013-15018.
[44] J. Lottersberger, S.A. Guerrero, G.G. Tonarelli, R. Frank, H. Tarabla, N.B. Vanasco, Epitope mapping of pathogenic Leptospira LipL32, Lett Appl Microbiol, 49 (2009) 641-645.
[45] J. Vaitukaitis, J.B. Robbins, E. Nieschlag, G.T. Ross, A method for producing specific antisera with small doses of immunogen, J Clin Endocrinol Metab, 33 (1971) 988-991.
[46] D.G. Arias, M.S. Cabeza, E.D. Erben, P.G. Carranza, H.D. Lujan, M.T. Tellez Inon, A.A. Iglesias, S.A. Guerrero, Functional characterization of methionine sulfoxide reductase A from Trypanosoma spp, Free Radic Biol Med, 50 (2011) 37-46.
[47] H.Y. Kim, V.N. Gladyshev, Methionine sulfoxide reduction in mammals: characterization of methionine-R-sulfoxide reductases, Mol Biol Cell, 15 (2004) 1055-1064.
[48] M. Hugo, L. Turell, B. Manta, H. Botti, G. Monteiro, L.E. Netto, B. Alvarez, R. Radi, M. Trujillo, Thiol and sulfenic acid oxidation of AhpE, the one-cysteine peroxiredoxin from Mycobacterium tuberculosis: kinetics, acidity constants, and conformational dynamics, Biochemistry, 48 (2009) 9416-9426.
[49] K. Johnsson, W.A. Froland, P.G. Schultz, Overexpression, purification, and characterization of the catalase-peroxidase KatG from Mycobacterium tuberculosis, J Biol Chem, 272 (1997) 2834-2840.
[50] D.T. Le, B.C. Lee, S.M. Marino, Y. Zhang, D.E. Fomenko, A. Kaya, E. Hacioglu, G.H. Kwak, A. Koc, H.Y. Kim, V.N. Gladyshev, Functional analysis of free methionine-R-sulfoxide reductases from Saccharomyces cerevisiae, J Biol Chem, 284 (2009) 4354-4364.
[51] D. Mumberg, R. Muller, M. Funk, Yeast vectors for the controlled expression of heterologous proteins in different genetic backgrounds, Gene, 156 (1995) 119-122.
[52] N. Eswar, B. Webb, M.A. Marti-Renom, M.S. Madhusudhan, D. Eramian, M.Y. Shen, U. Pieper, A. Sali, Comparative protein structure modeling using MODELLER, Curr Protoc Protein Sci, Chapter 2 (2007) Unit 2 9.
[53] M. Gouy, S. Guindon, O. Gascuel, SeaView version 4: A multiplatform graphical user interface for sequence alignment and phylogenetic tree building, Mol Biol Evol, 27 (2010) 221-224.
[54] E. Taherian, E. Mohammadi, A. Jahanian-Najafabadi, F. Moazen, V. Akbari, Cloning, Optimization of Periplasmic Expression and Purification of Recombinant Granulocyte Macrophage-Stimulating Factor in Escherichia coli BL21 (DE3), Adv Biomed Res, 8 (2019) 71.
[55] S. Boschi-Muller, G. Branlant, Methionine sulfoxide reductase: chemistry, substrate binding, recycling process and oxidase activity, Bioorg Chem, 57 (2014) 222-230.
[56] L. Tarrago, E. Laugier, M. Zaffagnini, C.H. Marchand, P. Le Marechal, S.D. Lemaire, P. Rey, Plant thioredoxin CDSP32 regenerates 1-cys methionine sulfoxide reductase B activity through the direct reduction of sulfenic acid, J Biol Chem, 285 (2010) 14964-14972.

[57] T.H. Lee, H.Y. Kim, An anaerobic bacterial MsrB model reveals catalytic mechanisms, advantages, and disadvantages provided by selenocysteine and cysteine in reduction of methionine-R-sulfoxide, Arch Biochem Biophys, 478 (2008) 175-180.
[58] H.Y. Kim, J.R. Kim, Thioredoxin as a reducing agent for mammalian methionine sulfoxide reductases B lacking resolving cysteine, Biochem Biophys Res Commun, 371 (2008) 490-494.
[59] L. Tarrago, E. Laugier, M. Zaffagnini, C. Marchand, P. Le Marechal, N. Rouhier, S.D. Lemaire, P. Rey, Regeneration mechanisms of Arabidopsis thaliana methionine sulfoxide reductases B by glutaredoxins and thioredoxins, J Biol Chem, 284 (2009) 18963-18971.
[60] B.C. Lee, V.N. Gladyshev, The biological significance of methionine sulfoxide stereochemistry, Free Radic Biol Med, 50 (2011) 221-227.
[61] E.H. Lee, K. Lee, G.H. Kwak, Y.S. Park, K.J. Lee, K.Y. Hwang, H.Y. Kim, Evidence for the dimerization-mediated catalysis of methionine sulfoxide reductase A from Clostridium oremlandii, PLoS One, 10 (2015) e0131523.
[62] K. Yoshida, A. Hara, K. Sugiura, Y. Fukaya, T. Hisabori, Thioredoxin-like2/2-Cys peroxiredoxin redox cascade supports oxidative thiol modulation in chloroplasts, Proc Natl Acad Sci U S A, 115 (2018) E8296-E8304.
[63] I. Braakman, L. Lamriben, G. van Zadelhoff, D.N. Hebert, Analysis of Disulfide Bond Formation, Curr Protoc Protein Sci, 90 (2017) 14.11.11-14.11.21.
[64] R.A. Kumar, A. Koc, R.L. Cerny, V.N. Gladyshev, Reaction mechanism, evolutionary analysis, and role of zinc in Drosophila methionine-R-sulfoxide reductase, J Biol Chem, 277 (2002) 37527-37535.
[65] P. Alamuri, R.J. Maier, Methionine sulfoxide reductase in Helicobacter pylori: interaction with methionine-rich proteins and stress-induced expression, J Bacteriol, 188 (2006) 5839-5850.
[66] L.G. Kuhns, M. Mahawar, J.S. Sharp, S. Benoit, R.J. Maier, Role of Helicobacter pylori methionine sulfoxide reductase in urease maturation, Biochem J, 450 (2013) 141-148.
[67] M. Mahawar, V. Tran, J.S. Sharp, R.J. Maier, Synergistic roles of Helicobacter pylori methionine sulfoxide reductase and GroEL in repairing oxidant-damaged catalase, J Biol Chem, 286 (2011) 19159-19169.
[68] M. Cinco, New insights into the pathogenicity of leptospires: evasion of host defences, New Microbiol, 33 (2010) 283-292.
[69] R. Murgia, R. Garcia, M. Cinco, Leptospires are killed in vitro by both oxygen-dependent and -independent reactions, Infect Immun, 70 (2002) 7172-7175.
[70] J. Moskovitz, V.K. Singh, J. Requena, B.J. Wilkinson, R.K. Jayaswal, E.R. Stadtman, Purification and characterization of methionine sulfoxide reductases from mouse and Staphylococcus aureus and their substrate stereospecificity, Biochem Biophys Res Commun, 290 (2002) 62-65.
[71] S. Boschi-Muller, S. Azza, G. Branlant, E. coli methionine sulfoxide reductase with a truncated N terminus or C terminus, or both, retains the ability to reduce methionine sulfoxide, Protein Sci, 10 (2001) 2272-2279.
[72] N. Rouhier, B. Kauffmann, F. Tete-Favier, P. Palladino, P. Gans, G. Branlant, J.P. Jacquot, S. Boschi-Muller, Functional and structural aspects of poplar cytosolic and plastidial type a methionine sulfoxide reductases, J Biol Chem, 282 (2007) 3367-3378.
[73] A. Olry, S. Boschi-Muller, G. Branlant, Kinetic characterization of the catalytic mechanism of methionine sulfoxide reductase B from Neisseria meningitidis, Biochemistry, 43 (2004) 11616-11622.

[74] M.A. Tossounian, B. Pedre, K. Wahni, H. Erdogan, D. Vertommen, I. Van Molle, J. Messens, Corynebacterium diphtheriae methionine sulfoxide reductase a exploits a unique mycothiol redox relay mechanism, J Biol Chem, 290 (2015) 11365-11375.
[75] M. Kantorow, W. Lee, D. Chauss, Focus on Molecules: methionine sulfoxide reductase A, Exp Eye Res, 100 (2012) 110-111.
[76] S. Boschi-Muller, A. Gand, G. Branlant, The methionine sulfoxide reductases: Catalysis and substrate specificities, Arch Biochem Biophys, 474 (2008) 266-273.
[77] N. Sasoni, D.M.L. Ferrero, S.A. Guerrero, A.A. Iglesias, D.G. Arias, First evidence of glutathione metabolism in Leptospira interrogans, Free Radic Biol Med, 143 (2019) 366-374.
[78] M. Saleh, S.G. Bartual, M.R. Abdullah, I. Jensch, T.M. Asmat, L. Petruschka, T. Pribyl, M. Gellert, C.H. Lillig, H. Antelmann, J.A. Hermoso, S. Hammerschmidt, Molecular architecture of Streptococcus pneumoniae surface thioredoxin-fold lipoproteins crucial for extracellular oxidative stress resistance and maintenance of virulence, EMBO Mol Med, 5 (2013) 1852-1870.
[79] V.K. Singh, K. Singh, K. Baum, The Role of Methionine Sulfoxide Reductases in Oxidative Stress Tolerance and Virulence of Staphylococcus aureus and Other Bacteria, Antioxidants (Basel), 7 (2018).
[80] V.K. Singh, M. Vaish, T.R. Johansson, K.R. Baum, R.P. Ring, S. Singh, S.K. Shukla, J. Moskovitz, Significance of four methionine sulfoxide reductases in Staphylococcus aureus, PLoS One, 10 (2015) e0117574.
[81] S. Boschi-Muller, Molecular Mechanisms of the Methionine Sulfoxide Reductase System from Neisseria meningitidis, Antioxidants (Basel), 7 (2018).
[82] M. Lo, G.L. Murray, C.A. Khoo, D.A. Haake, R.L. Zuerner, B. Adler, Transcriptional response of Leptospira interrogans to iron limitation and characterization of a PerR homolog, Infect Immun, 78 (2010) 4850-4859.
[83] R.E. Corin, C.D. Cox, Characterization of leptospiral catalase and peroxidase, Can J Microbiol, 26 (1980) 121-129.
[84] M.J. Gray, W.Y. Wholey, U. Jakob, Bacterial responses to reactive chlorine species, Annu Rev Microbiol, 67 (2013) 141-160.
[85] N. Makukhin, V. Havelka, L. Polachova, P. Rampirova, V. Tarallo, K. Strisovsky, J. Misek, Resolving oxidative damage to methionine by an unexpected membrane-associated stereoselective reductase discovered using chiral fluorescent probes, FEBS J, 286 (2019) 4024-4035.
[86] A. Gennaris, B. Ezraty, C. Henry, R. Agrebi, A. Vergnes, E. Oheix, J. Bos, P. Leverrier, L. Espinosa, J. Szewczyk, D. Vertommen, O. Iranzo, J.F. Collet, F. Barras, Repairing oxidized proteins in the bacterial envelope using respiratory chain electrons, Nature, 528 (2015) 409-412.
[87] C. Andrieu, A. Vergnes, L. Loiseau, L. Aussel, B. Ezraty, Characterisation of the periplasmic methionine sulfoxide reductase (MsrP) from Salmonella Typhimurium, Free Radic Biol Med, (2020).

<u>Figure 1:</u> Alignment of *Lin*MsrB amino acid sequence with MsrB from other sources. The sequences stacked together with MsrB from *L. interrogans* correspond to MsrB from *L. biflexa* (NCBI_WP_012388169.1), *E. coli* (NCBI_WP_001284612.1), *Homo sapiens* (NCBI_EAW97151.1), *Mus musculus* (NCBI_NP_796066.1), *Mycobacterium tuberculosis* (NCBI_WP_040631412.1) and *Trypanosoma cruzi*

(NCBI_XP_817746.1). The boxes with a full line border show the CXXC motifs necessary to ion metal bind. The box with a dashed line border points out the redox-active site with the nucleophilic Cys marked by the arrow. The alignment was performed using the ClustalX program.

Figure 2: Phylogenetic analysis of MsrB proteins. The phylogenetic tree was arranged using the Neighbor-Joining method (bootstrap of 10,000), as described in the Material and Methods section. *Lin*MsrB (number 15, asterisk) is grouped with proteins containing the CA(G/A)C within the first motif used for the metal-binding (violet lines). Within this group, *Lin*MsrB diverges early next to the *Acidobacterium capsulatum* protein (number 01). Yellow lines: CVCC-containing proteins. Red lines: CL(V/I)C-containing proteins. Turquoise lines: CI(G/C)C-containing proteins. Gray lines: non-metal binding Msr sequences. AB, MsrAB. Pb: proteobacteria. Acidob: acidobacteria.

Figure 3: Alignment of *Lin*MsAs amino acid sequence with MsrA from other sources. The sequences stacked together with MsrAs from *L. interrogans* correspond to MsrA from *Bacillus subtilis* (NCBI-AAY97801.1), *Bos taurus* (NCBI-AAI02981.1), *E. coli* (NCBI-AAA97115.1), *Homo sapiens* (NCBI-NP_036463), *L. biflexa* (NCBI-WP_012389572.1 and NCBI-WP_012389852.1), *Mycobacterium tuberculosis* (NCBI-P0A5L0.1) and *Rhodobacter capsulatus* (NCBI-KQB14835.1), respectively. The box indicates the redox-active site, which is conserved between MsrAs. Notice that Msrs from pathogen and saprophyte *Leptospira* strains analyzed contain the redox-active site is of the kind CXXC. The arrows point out other Cys residues common between the sequences present in the alignment. The alignment was performed using the ClustalX program.

Figure 4: Phylogenetic analysis of MsrA proteins. The phylogenetic tree was constructed using the Neighbor-Joining method (bootstrap of 10,000), as described in the Material and Methods section. Two main branches can be observed: one comprising prokaryotic MsrAB sequences and a second larger one formed by three subgroups. *Lin*MsrA1 (sequence number 8) clusters with other protein from the Spirochaetes phylum (sequence number 7, *L. biflexa*), whereas *Lin*MsrA2 (sequence number 9) groups with further prokaryotic organisms. Turqouise lines: proteins harbour the sequence motif GCFWC. Red lines: proteins harbour the sequence motif GCFWG. A1:

MsrA1. A2: MsrA2. AB, MsrAB. Pb: proteobacteria. Actinob: actinobacteria. Cyanob: cyanobacteria.

Figure 5: Evaluation of the reaction products by TLC. The reaction mixtures are detailed in the tables below each chromatographic migration profile. The stationary phase used was aluminum-coated silica, and the mobile phase was butanol:acetic acid:water (60:15:25). The plate was revealed with ninhydrin spray.

Figure 6: Functionality of *Lin*Msrs *in vivo*. *S. cerevisiae* strain GY202 was transformed with the p425 plasmid empty vector, [p425/*Lin*MsrB], [p425/*Lin*MsrA1], and with [p425/*Lin*MsrA2]. Cells were plated on SD-agar (defined medium), containing 100 µM L-Met, 100 µM racemic L-MetSO, or 100 µM L-Met(*S*)SO. The initial densities were normalized to $5{\cdot}10^6$ cell ml^{-1} and incubated at 28 °C between 48-72 h.

Figure 7: Sensitivity of recombinant *S. cerevisiae* strains to exogenous oxidizing agents. The parental strain W303-1B of *S. cerevisiae* was transformed with the empty p425 plasmid, whereas the strain GY202 (triple mutant) was transformed with the empty p425 plasmid, or with [p425/*Lin*MsrB], [p425/*Lin*MsrA1], or [p425/*Lin*MsrA2]. The cells were normalized ($5{\cdot}10^6$ cell ml^{-1}) and incubated at 28 °C for 1 h in the presence or absence of oxidizing agents such as H_2O_2 and HClO. After that time, serial 1/5 dilutions were made, and finally, 10 µl of each dilution was deposited on YPD agar (complex medium). The plates were incubated at 28 ° C for 48 to 72 h.

Figure 8: Msr activity of *L. interrognas* enzymes on MetSO-proteins. The Msr activity was measured by monitoring NADPH oxidation at 340 nm using a coupled assay at 30 °C. For MsrA enzymes, the reaction mixture contained 100 mM potassium phosphate, pH 7.0, 2 mM EDTA, 300 µM NADPH, 1 µM *Lin*TrxR; 10 µM *Lin*Trx, and different concentrations of *Lin*MsrAs. For MsrB enzyme, the reaction mixture contained 100 mM potassium phosphate, pH 7.0, 2 mM EDTA, 300 µM NADPH, 1 U ml^{-1} *Sacharomyces cerevisiae* glutathione reductase; 10 µM *Hsa*Grx (plus 3 mM GSH), and different concentrations of *Lin*MsrB. Reactions began by the addition of 0.1 $\mu g{\cdot}\mu l^{-1}$ processed total soluble protein extract (derived from *L. interrogans* cells stressed or not with HClO). The derivative of unstressed *L. interrogans* was used as the total soluble

protein extract of reference. The processing of total soluble protein extracts as detailed in materials and methods. The objective of the treatment (reduction and subsequent alkylation) of the total protein extracts is to eliminate all potentially reactive forms of cysteine residues (oxidized forms, outlined in the figure) in proteins with the coupled enzyme system. S-CAM: cysteine alkylated with iodoacetamide.

Figure 9: Oxidation-reduction assay of *Lin*Msrs visualized by non-reducing SDS-PAGE. *Lin*MsrA1, *Lin*MsrA1C25S, *Lin*MsrA2, *Lin*MsrA2C18S or *Lin*MsrB (10 μM each one) were oxidized with 10 mM L-MetSO or reduced with 10 mM DTT, for 10 min at 30 °C. After this incubation the proteins were visualized in a 15% non-reducing SDS-PAGE.

Figure 10: Tridimensional model of *Lin*Msrs. The building of the structure models was based on a template derived from a known X-ray structure of the orthologous Msrs from: *Escherichia coli* (PDB 1FF3) and *Populus trichocarpa* (PDB 2J89) for *Lin*MsrA1 for **(A)** and *Lin*MsrA2 **(B)**; *Bacillus subtilis* (PDB 3E0O), *Methanothermobacter thermautotrophicus* (PDB 2K8D), *Mus musculus* (PDB 2L1U), *Neisseria meningitidis* (PDB 3HCG), *Treponema denticola* (PDB 5FA9), *Burkholderia pseudomallei* (PDB 3CXK), *Streptococcus pneumoniae* (PDB 3E0M) and *Xanthomonas campestris* (PDB 3HCJ) for *Lin*MsrB for **(C)**. The global Verify-3D averaged 3D1D scores of 63.41 for *Lin*MsrA1, 67.13 for *Lin*MsrA2 and 59 for *Lin*MsrB, indicate that our best models were in between the range of well-predicted structures.

Figure 11: Identification of Msrs in *L. interrogans* protein extracts. A pool of three *L. interrogans* cell cultures in the exponential phase was resuspended in 1 ml of a solution composed of 50 mM Tris-HCl pH 8.0; 100 mM NaCl and protease inhibitor cocktail SET III (Lysis buffer). The cell suspension was sonicated and then centrifuged at 21,000 *xg* by 30 min at 4 °C. The supernatant obtained represents the soluble fraction in the panel. The obtained pellet after sonication was washing with Lysis buffer and then dissolved with Lysis buffer plus NP-40 1% (v/v). The obtained dissolution was named membrane fraction. Both cell fractions were analyzed by western blot using specific polyclonal antibodies against different proteins: *Lin*MsrB (diluted 1/1000), *Tcr*MsrA (diluted 1/1000), *Lin*Lp32 (diluted 1/25000), and *Lin*TrxR (diluted 1/1000).

We employed HRP-conjugated anti-rabbit as a secondary antibody and visualized the bands using the ECL Western blotting detections reagents.

Figure 12: Digitonin titration of *Lin*Msrs in *L. interrogans* cells. A cellular pellet from a culture of 24 ml of *L. interrogans* (in the exponential growth phase) of $OD_{420\ nm}$ of 0.23 was treated successively with increasing concentrations of digitonin (from 0 to 4 mg ml^{-1}) in extraction buffer (20 mM Tris-HCl, 100 mM NaCl, 1 mM EDTA and 250 mM sucrose, pH 7.5). Protein fractions in the supernatants were subjected to SDS-PAGE and western blot analysis. Polyclonal antibodies against *Lin*MsrA and *Lin*MsrB allowed to identify the respective protein, *Lin*TrxR, and *Lin*AhpC were the cytoplasmic markers, and *Lin*catalase the periplasmic marker.

Figure 13: Msr-dependent catalase activity recovery assay. The enzyme was subjected to two successive incubation steps at 30 °C and pH 7.0. First, it was incubated with HClO, then with *Lin*MsrAs or *Lin*MsrB, and finally, catalase activity was measured by following the consumption of H_2O_2 at 240 nm. The *Lin*Trx system was the reducing system for *Lin*MsrAs, and the GSH/Grx redox pair was the reducer of *Lin*MsrB. Values of activity were reported as relative to that of untreated-catalase.

Figure 14: A) The proposed reaction mechanism for *Lin*MsrAs catalysis. The thiolate group of catalytic Cys of *Lin*MsrAs (I) attacks the sulfoxide moiety of Met(*S*)SO and forms the sulfenic acid intermediate (II), with the concomitant release of Met. The catalytic Cys sulfenic acid (II) is attacked by the vicinal resolutive Cys residue and generate a vicinal disulfide intermediate (III). The vicinal disulfide bond in the *Lin*MsrAs (III) is attacked by the resolutive Cys in the C-terminal leading to the resolutive disulfide bond isomerization and the concomitant generation of a partially reduced form of *Lin*MsrA (IV). The partially reduced form of *Lin*MsrAs (IV) can react with other Met(S)SO molecule to generate the full oxidized form of *Lin*MsrAs (V) or could be reduced by the Trx in the resolutive disulfide bond, thus regenerating the fully reduced form of *Lin*MsrAs (I). The full oxidized form of *Lin*MsrAs (V) could be partially reduced by the Trx in the resolutive disulfide bond, thus generating the sulfenic acid intermediate of *Lin*MsrAs (II).

B) The proposed catalytic mechanism of *Lin*MsrB. The thiolate group of catalytic Cys of *Lin*MsrB (I) attacks the sulfoxide moiety of Met(*R*)SO and forms the sulfenic

acid intermediate (II), with the concomitant release of Met. The Cys sulfenic acid intermediate (II) is attacked by the GSH molecule and generate a glutathionylated MsrB intermediate (III). The mixed disulfide bond in the *Lin*MsrB (III) is resolving by the Grx, leading to the formation of reduced *Lin*MsrB (thiolate form, I). Alternatively, the sulfenic acid intermediate of *Lin*MsrB (II) could be directly reduced by the Trx, thus regenerating the thiolate form of *Lin*MsrB (I).

Gene	Primer	Restriction site	*T*m (°C)
*linmsra*1Fow	**GGATCC**ATGCAACCTTTGGATTCTAAG	*Bam*HI	68
*linmsra*1Rev	**CTCGAG**TTAATTTGTGCTTTTGACTTT	*Xho*I	54
*linmsra*2$_{SP}$Fow	**GGATTC**ATGTTTAATCTTAAAATTTTAATTTT	*Bam*HI	57
*linmsra*2Fow	**CATATG**GCGACTCCTAAAAGAGAA	*Nde*I	65
*linmsra*2Rev	**CTCGAG**TTAACGTTGCCTACAGATTTT	*Xho*I	57
linmsrb$_{SP}$*Fow*	**CATATG**AAAAACAACATTTTACTC	*Nde*I	47
*linmsrb*Fow	**CATATG**AATTACGAAGTCAACAAA	*Nde*I	49
*linmsrb*Rev	**CTCGAG**TTCTTTCTGAAACTTTAAGGA	*Xho*I	55
*linmsra1*C25SFow	GCGGTTGTTTTTGGTCTCTCGAAGCGGTATATC	---	78
*linmsra1*C25SRev	GATATACCGCTTCGAGAGACCAAAAACAACCGC	---	78
*linmsra2*C18SFow	CGGCGGTTGTTTTTCGCTCTATGGAAGGACCATTCG	---	80
*linmsra2*C18SRev	CGAATGGTCCTTCCATAGACCAAAAACAACCGCCG	---	80

Table 1: Primers used for PCR amplification of the genes encoding for methionine sulfoxide reductases of *L. interrogans* (*Lin*MsrA1, *Lin*MsrA1C25S, *Lin*MsrA2$_{SP}$, *Lin*MsrA2, *Lin*MsrA2C18S, *Lin*MsrB$_{SP}$ and *Lin*MsrB). The restriction sites included are in bold and underlined.

Enzyme	Substrate	Co-substrate	$k_{cat\ app}$ (min^{-1})	Km_{app} (μM)	$k_{cat}\,Km^{-1}$ (M^{-1} s^{-1})
***Lin*MsrB**	L-Met(*R*)SO	25 μM *Hsa*Grx	0.46 ± 0.03	1000 ± 100	8.0
	N-AcMet(*R*)SO	25 μM *Hsa*Grx	0.85 ± 0.04	210 ± 20	$6.7{\cdot}10^{1}$
		*Lin*Trx	2.5 mM N-AcMet(*R*)SO	0.26 ± 0.02	26 ± 4	$1.7{\cdot}10^{2}$
		*Hsa*Grx	2.5 mM N-AcMet(*R*)SO	0.87 ± 0.04	2.8 ± 0.3	$5.2{\cdot}10^{3}$
***Lin*MsrA1**	L-Met(*S*)SO	20 μM *Lin*Trx	23.3 ± 0.5	550 ± 40	$7.1{\cdot}10^{2}$

	*Lin*Trx	2.5 mM L-Met(*S*)SO	30.5 ± 0.9	10.1 ± 0.6	$5.0 \cdot 10^4$
	N-AcMet(*S*)SO	20 μM *Lin*Trx	24.9 ± 0.9	2700 ± 200	$1.5 \cdot 10^2$
	*Lin*Trx	2.5 mM N-AcMet(*S*)SO	19.0 ± 0.6	8.1 ± 0.5	$4.0 \cdot 10^4$
***Lin*MsrA1C25S**	L-Met(*S*)SO	20 μM *Lin*Trx	0.327 ± 0.005	135 ± 8	$4.0 \cdot 10^1$
	*Lin*Trx	2.5 mM L-Met(*S*)SO	N.D.	>>20	$3.2 \cdot 10^2$
	N-AcMet(*S*)SO	20 μM *Lin*Trx	0.329 ± 0.008	280 ± 20	$2.0 \cdot 10^1$
	*Lin*Trx	2.5 mM N-AcMet(*S*)SO	N.D.	>>20	$4.0 \cdot 10^2$
***Lin*MsrA2**	L-Met(*S*)SO	20 μM *Lin*Trx	5.9 ± 0.1	390 ± 20	$2.5 \cdot 10^2$
	*Lin*Trx	2.5 mM L-Met(*S*)SO	5.0 ± 0.3	2.0 ± 0.2	$4.2 \cdot 10^4$
	N-AcMet(*S*)SO	20 μM *Lin*Trx	12.2 ± 0.2	1400 ± 100	$1.4 \cdot 10^2$
	*Lin*Trx	2.5 mM N-AcMet(*S*)SO	6.1 ± 0.1	1.8 ± 0.3	$5.6 \cdot 10^4$
***Lin*MsrA2C18S**	$k_{cat\ app}$ = 0.008 ± 0.003 min^{-1} [with 20 μM *Lin*Trx and 2.5 mM L-Met(*S*)SO]				

Table 2: Apparent kinetic parameters of *Lin*Msrs. The measurements were performed at pH 7.0 and 30 °C. N.D. = not determinable. The reaction mixture composition is detailed in Material and Methods. Steady-state kinetics analysis was performed using 0.1 to 5 mM L-MetSO or N-AcMetSO, 0.1 to 40 μM *Lin*Trx (plus 2 μM *Lin*TrxR) or *Hsa*Grx (plus 3 mM GSH) and 1 μM *Lin*MsrA1, or 1 μM *Lin*MsrA2, or 12 μM *Lin*MsrA1C25S, or 10 μM *Lin*MsrB.

Enzyme	Total Cys (from sequence)	[R-SH]/[Msr] (full reduced)	[R-SH]/[Msr] (after MetSO treatment)	[R-SOH]/[Msr] (after MetSO treatment)
***Lin*MsrA1**	5	4.9 ± 0.2	2.6 ± 0.3[#] 1.8 ± 0.1[*]	0.12 ± 0.04[#] 0.8 ± 0.3[*]
***Lin*MsrA1C25S**	4	3.9 ± 0.4	3.1 ± 0.2[#]	0.9 ± 0.4[#]
***Lin*MsrA2**	3	3.0 ± 0.3	0.9 ± 0.3[#] 0.03 ± 0.01[*]	0.10 ± 0.05[#] 0.89 ± 0.08[*]
***Lin*MsrA2C18S**	2	1.9 ± 0.5	1.2 ± 0.3[#]	0.7 ± 0.5[#]
***Lin*MsrB**	5	1.1 ± 0.3	0.3 ± 0.1[#]	0.8 ± 0.2[#]

Table 3: Titration of thiol and sulfenic acid moieties in *Lin*Msrs. The proteins were incubated with 25 mM DTT for 15 min at 25 °C and pH 7.5. After desalting (using gel filtration chromatography with Sephadex-G25), the proteins were incubated with

L-Met(*S*)SO or L-Met(*R*)SO (according to the evaluated Msr) at Msr:MetSO molar ratios of 1:50 (#) or 1:500 (*) for 15 min at 25 °C and pH 7.5. After that, the remained sulfoxide was eliminated with gel filtration chromatography, and the content of thiol (R-SH, with DTNB reagent) or sulfenic acid (R-SOH, with NBD-HCl reagent) groups was determined in the different proteins as described in Materials and methods.

Highlights

- *Lin*MsrB catalyzed the reduction of Met(*R*)SO using Grx or Trx as substrates.
- *Lin*MsrAs reduced Met(*S*)SO using the homologous Trx system.
- *Lin*MsrAs present a vicinal resolutive Cys residue in their active sites.
- *Lin*MsrB was able to revert the *in vitro* HClO-dependent inactivation of catalase.
- *Lin*Msrs show cytoplasmic and periplasmic localization in *L. interrogans*.

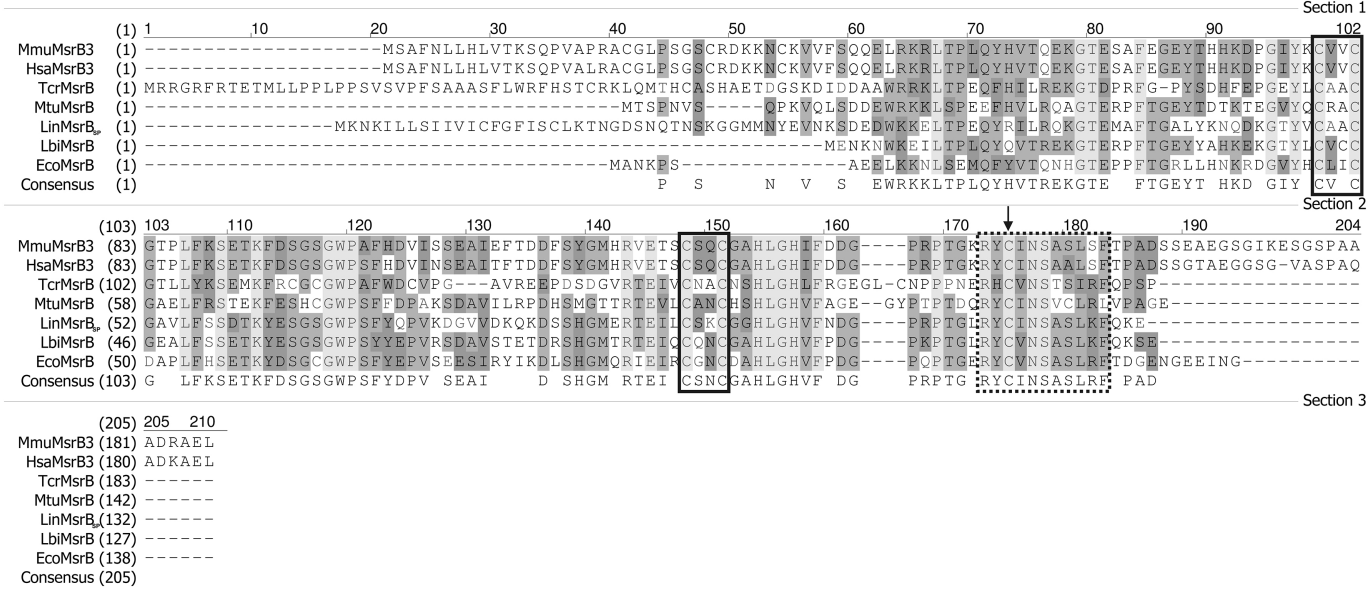
Section 1
Section 2
Section 3
MmuMsrB3
HsaMsrB3
TcrMsrB
MtuMsrB
LinMsrB∞
LbiMsrB
EcoMsrB
Consensus

Figure 1

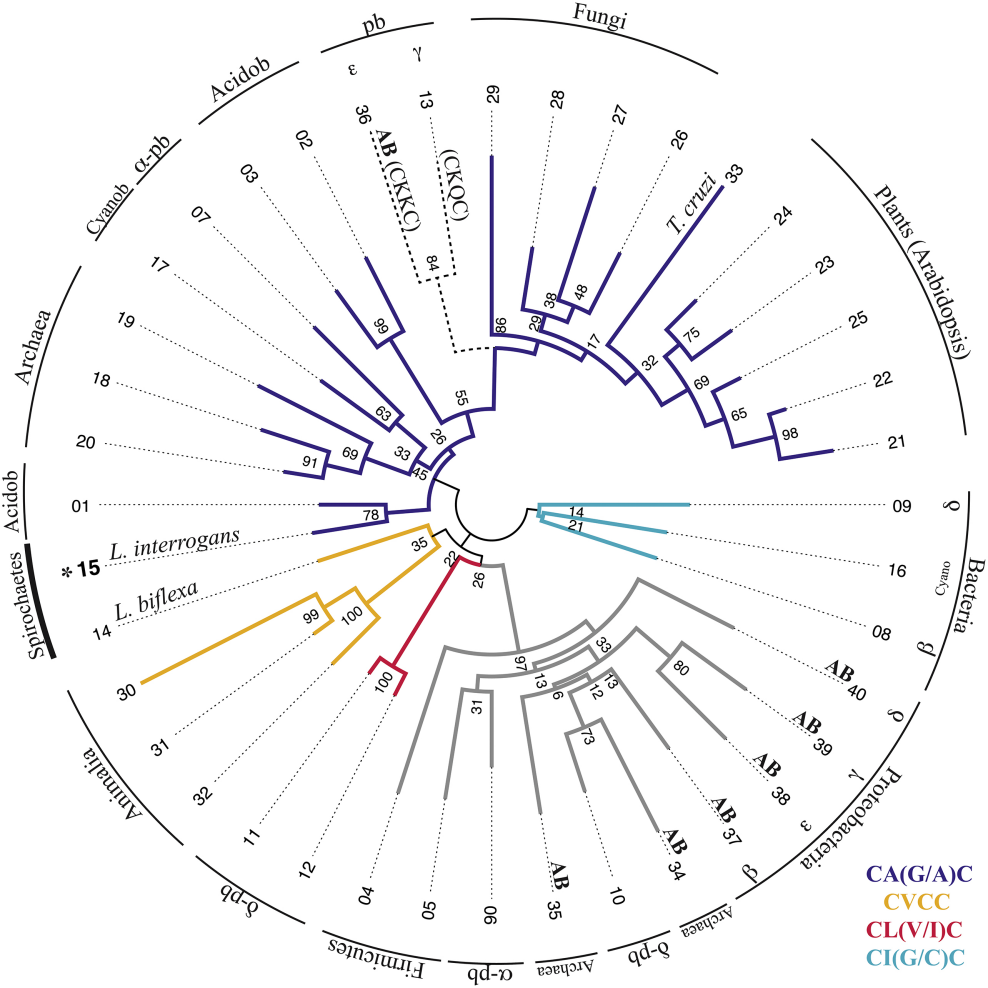
Fungi
Plants (Arabidopsis)
Bacteria
Archaea
Animalia
Spirochaetes
Acidob
Cyanob
α-pb
pb
Acidob
ε
γ
(CKQC)
AB (CKKC)
T. cruzi
L. interrogans
L. biflexa
* 15
δ
Cyano
β
δ
γ
ε
β
Archaea
δ-pb
Archaea
α-pb
Firmicutes
δ-pb
Proteobacteria
AB 40
AB 39
AB 38
AB 37
AB 34
AB 35
CA(G/A)C
CVCC
CL(V/I)C
CI(G/C)C

Figure 2

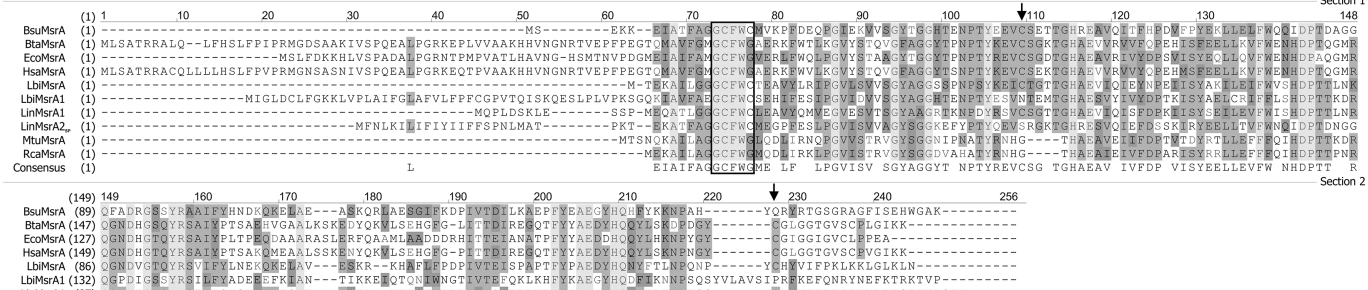
Section 1
Section 2
BsuMsrA
BtaMsrA
EcoMsrA
HsaMsrA
LbiMsrA
LbiMsrA1
LinMsrA1
LinMsrA2
MtuMsrA
RcaMsrA
Consensus

Figure 3

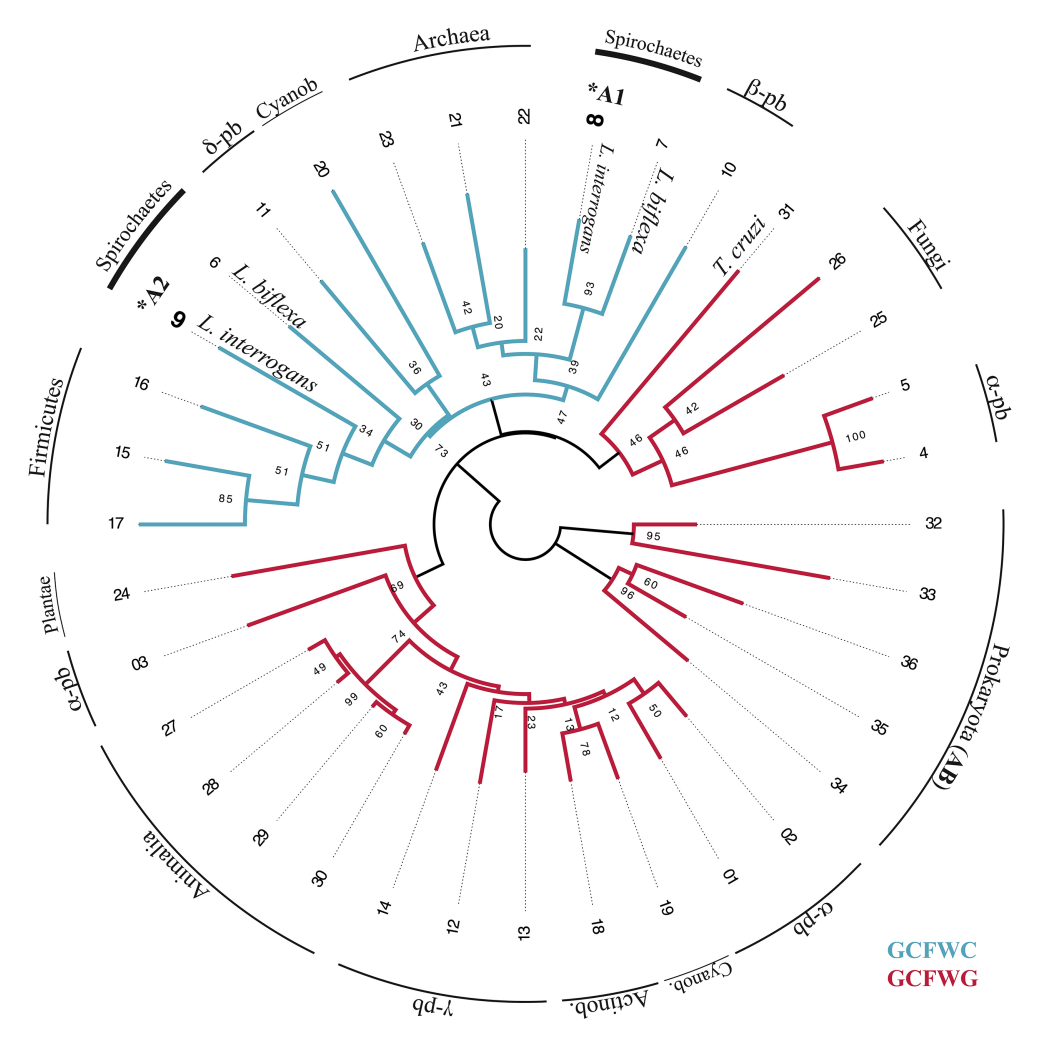
Archaea
Spirochaetes
β-pb
Fungi
α-pb
Prokaryota (AB)
α-pb
γ-pb
δ-pb
Cyanob
Spirochaetes
Firmicutes
Plantae
Animalia
Cyanob.
Actinob.
*A1
*A2
L. interrogans
L. biflexa
T. cruzi
GCFWC
GCFWG

Figure 4

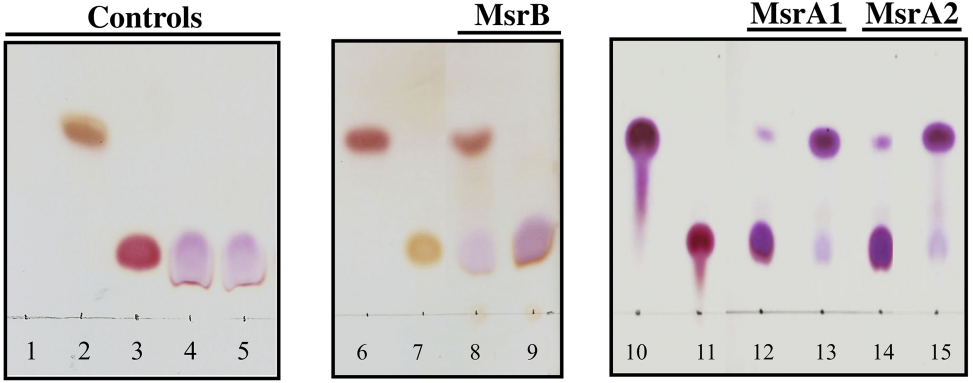

	1	2	3	4	5	6	7	8	9	10	11	12	13	14	15
***Lin*Msr**	-	-	-	-	-	-	-	✓	✓	-	-	✓	✓	✓	✓
DTT	✓	-	-	-	-	✓	✓	✓	✓	✓	✓	✓	✓	✓	✓
L-Met	-	✓	-	-	-	✓	-	-	-	✓	-	-	-	-	-
L-MetSO	-	-	✓	-	-	-	✓	-	-	-	✓	-	-	-	-
L-Met(*R*)SO	-	-	-	✓	-	-	-	✓	-	-	-	✓	-	✓	-
L-Met(*S*)SO	-	-	-	-	✓	-	-	-	✓	-	-	-	✓	-	✓
Phosphate buffer	✓	✓	✓	✓	✓	✓	✓	✓	✓	✓	✓	✓	✓	✓	✓

Figure 5

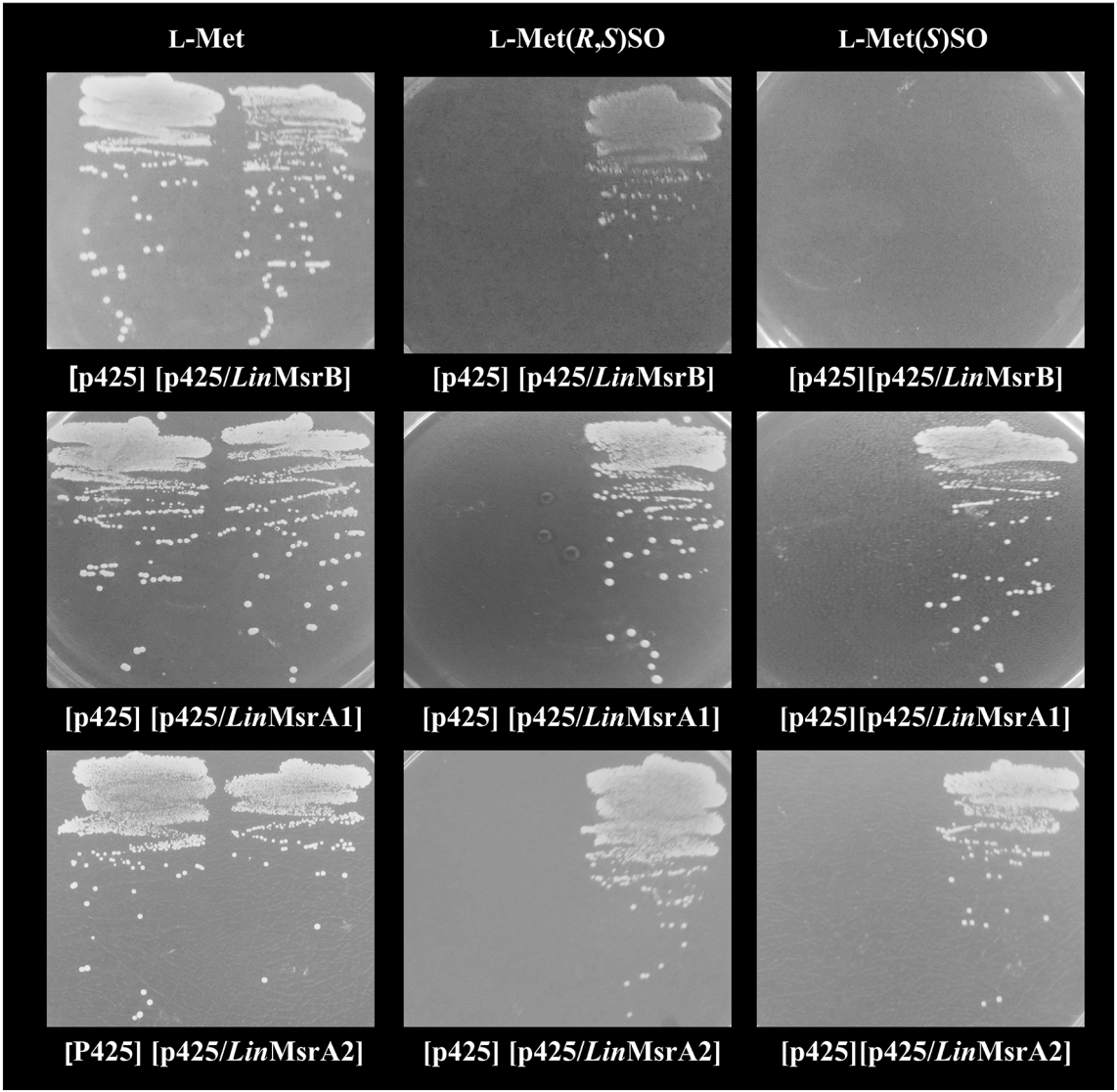
L-Met
L-Met(*R*,*S*)SO
L-Met(*S*)SO
[p425] [p425/*Lin*MsrB]
[p425] [p425/*Lin*MsrB]
[p425][p425/*Lin*MsrB]
[p425] [p425/*Lin*MsrA1]
[p425] [p425/*Lin*MsrA1]
[p425][p425/*Lin*MsrA1]
[P425] [p425/*Lin*MsrA2]
[p425] [p425/*Lin*MsrA2]
[p425][p425/*Lin*MsrA2]

Figure 6

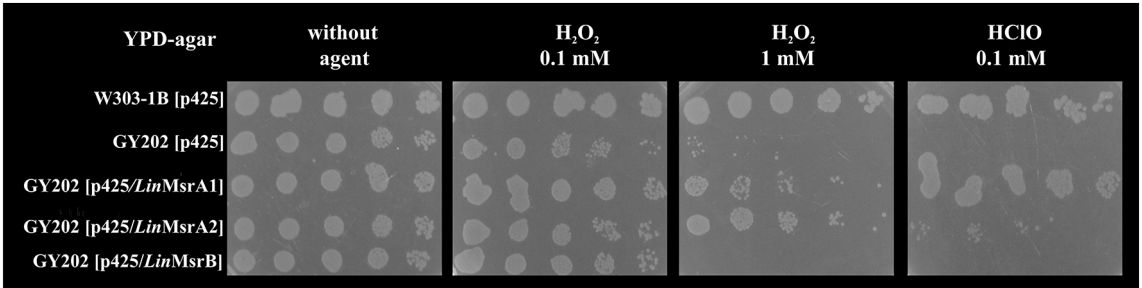
YPD-agar
without agent
H_2O_2 0.1 mM
H_2O_2 1 mM
HClO 0.1 mM
W303-1B [p425]
GY202 [p425]
GY202 [p425/*Lin*MsrA1]
GY202 [p425/*Lin*MsrA2]
GY202 [p425/*Lin*MsrB]

Figure 7

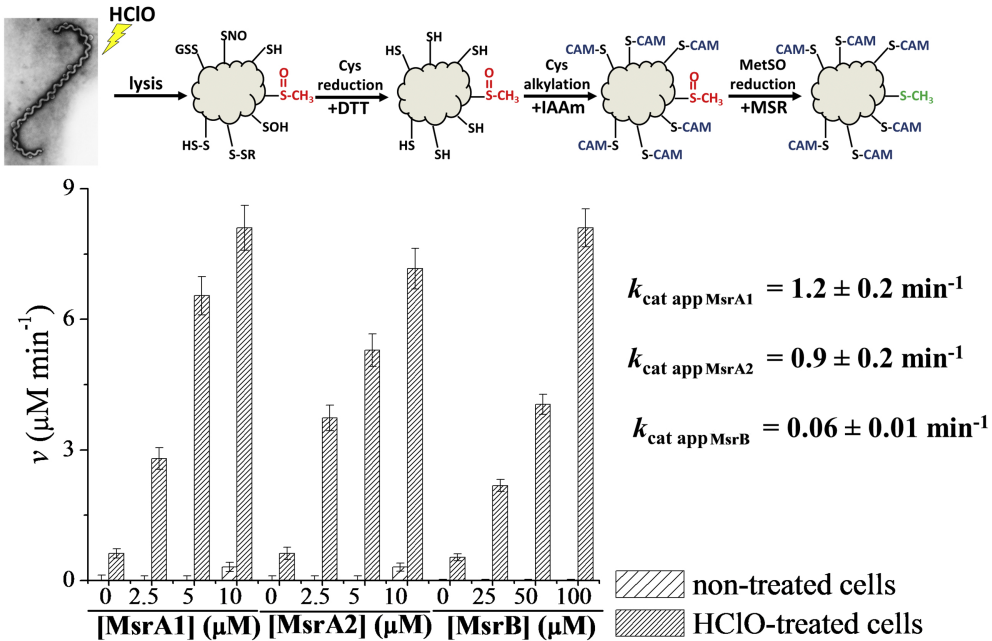
HClO
lysis
GSS
SNO
SH
HS-S
S-SR
SOH
S-CH3
Cys
reduction
+DTT
HS
SH
Cys
alkylation
+IAAm
CAM-S
S-CAM
MetSO
reduction
+MSR
v (μM min-1)
9
6
3
0
0
2.5
5
10
25
50
100
[MsrA1] (μM)
[MsrA2] (μM)
[MsrB] (μM)
non-treated cells
HClO-treated cells
kcat app MsrA1 = 1.2 ± 0.2 min-1
kcat app MsrA2 = 0.9 ± 0.2 min-1
kcat app MsrB = 0.06 ± 0.01 min-1

Figure 8

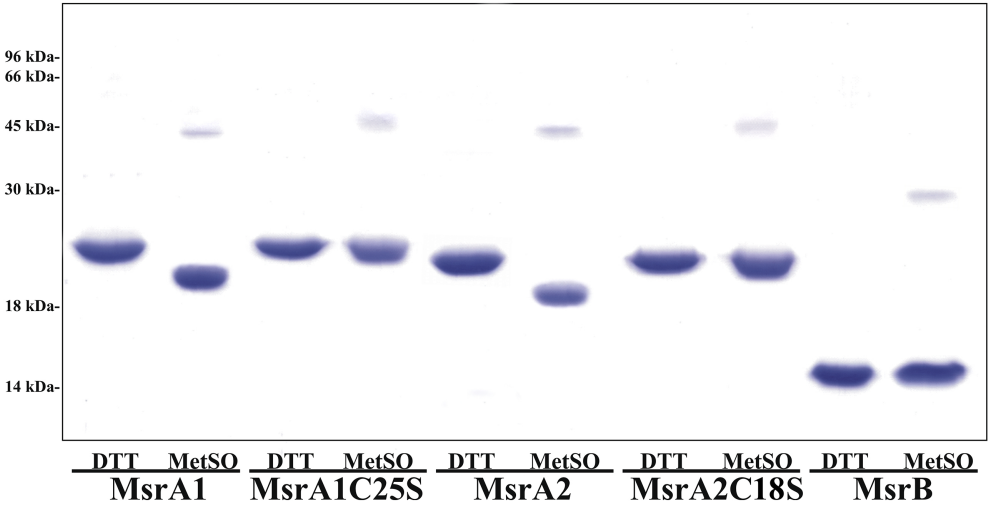
96 kDa-
66 kDa-
45 kDa-
30 kDa-
18 kDa-
14 kDa-
DTT MetSO
MsrA1
DTT MetSO
MsrA1C25S
DTT MetSO
MsrA2
DTT MetSO
MsrA2C18S
DTT MetSO
MsrB

Figure 9

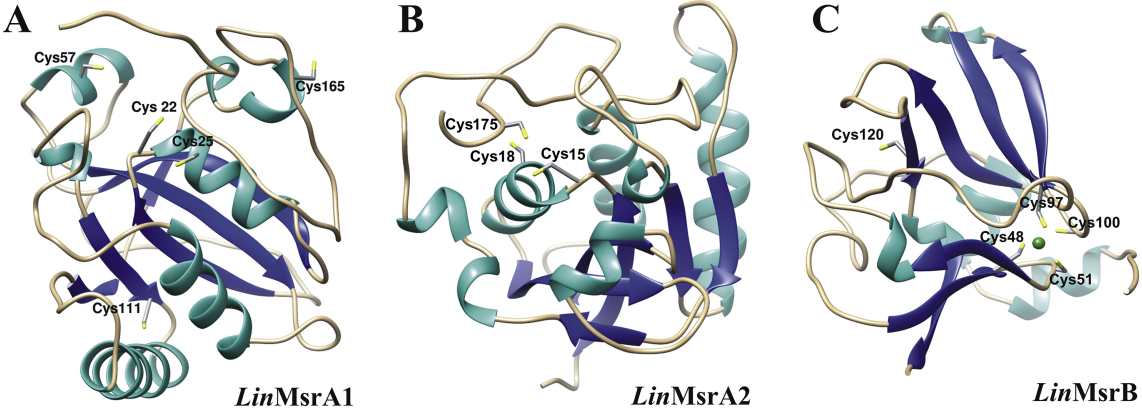
A
Cys57
Cys 22
Cys25
Cys165
Cys111
LinMsrA1
B
Cys175
Cys18
Cys15
LinMsrA2
C
Cys120
Cys97
Cys100
Cys48
Cys51
LinMsrB

Figure 10

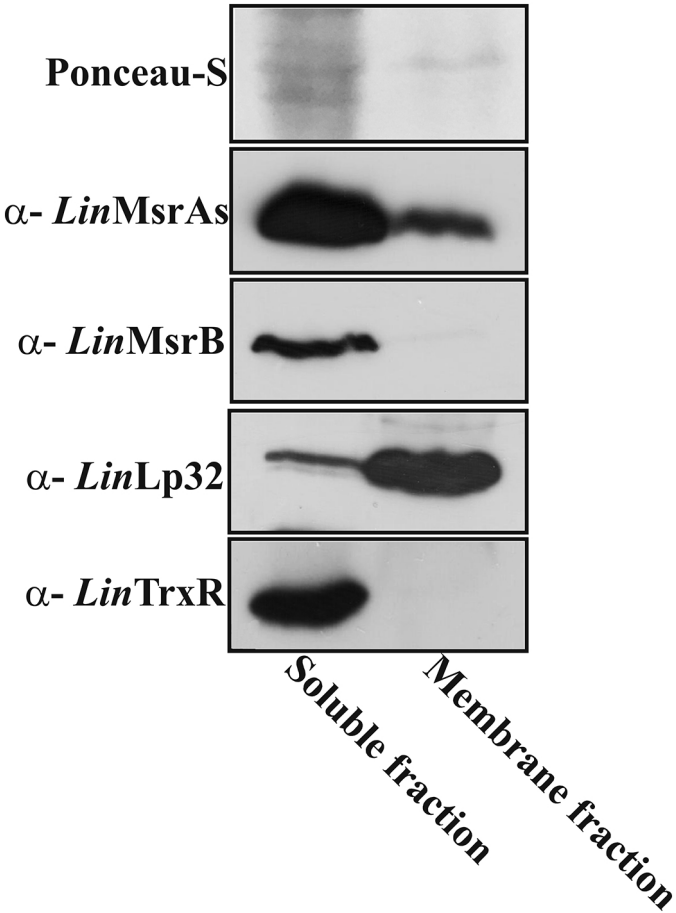
Ponceau-S
α- LinMsrAs
α- LinMsrB
α- LinLp32
α- LinTrxR
Soluble fraction
Membrane fraction

Figure 11

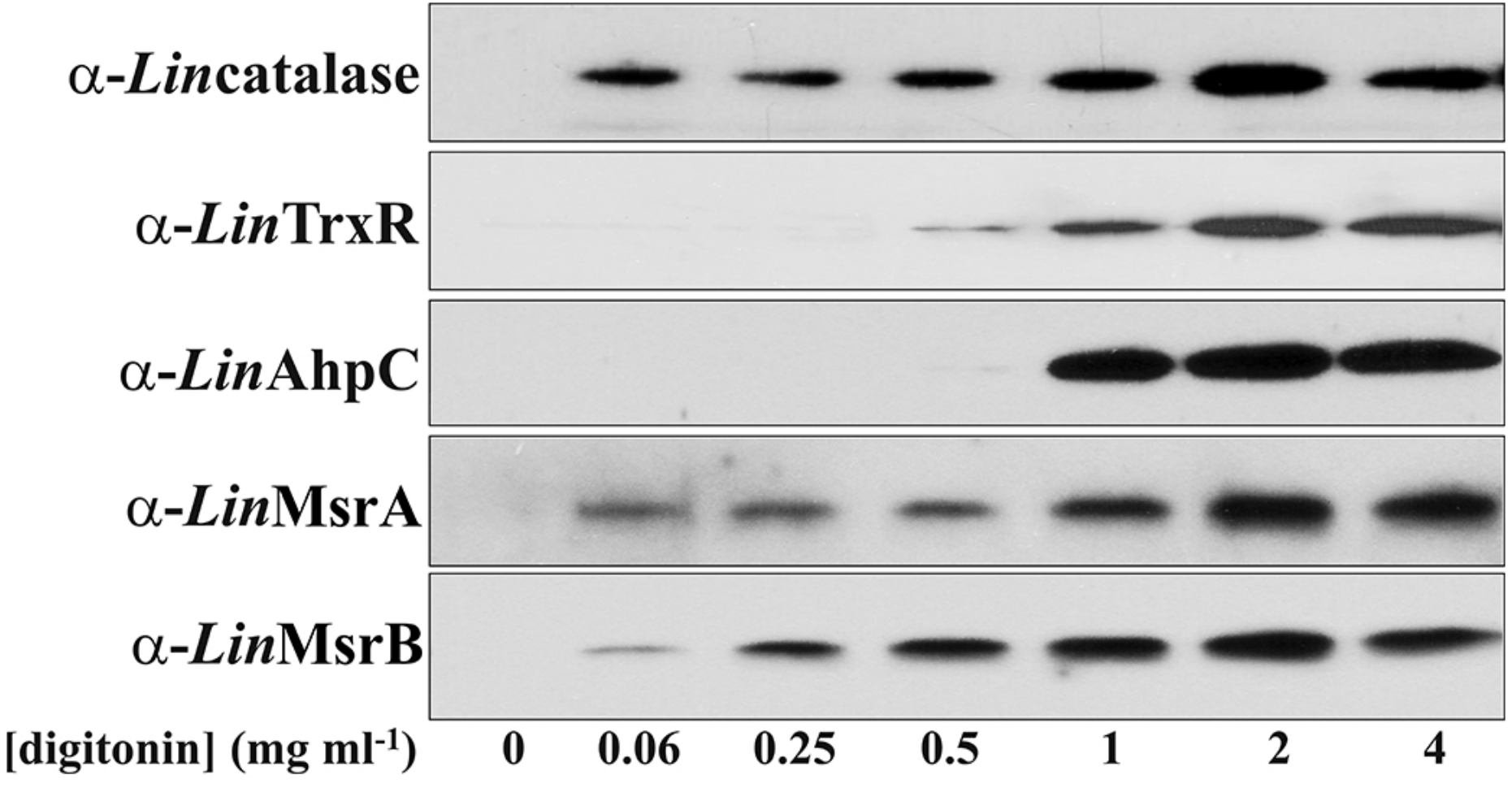
α-*Lin*catalase
α-*Lin*TrxR
α-*Lin*AhpC
α-*Lin*MsrA
α-*Lin*MsrB
[digitonin] (mg ml^{-1})
0
0.06
0.25
0.5
1
2
4

Figure 12

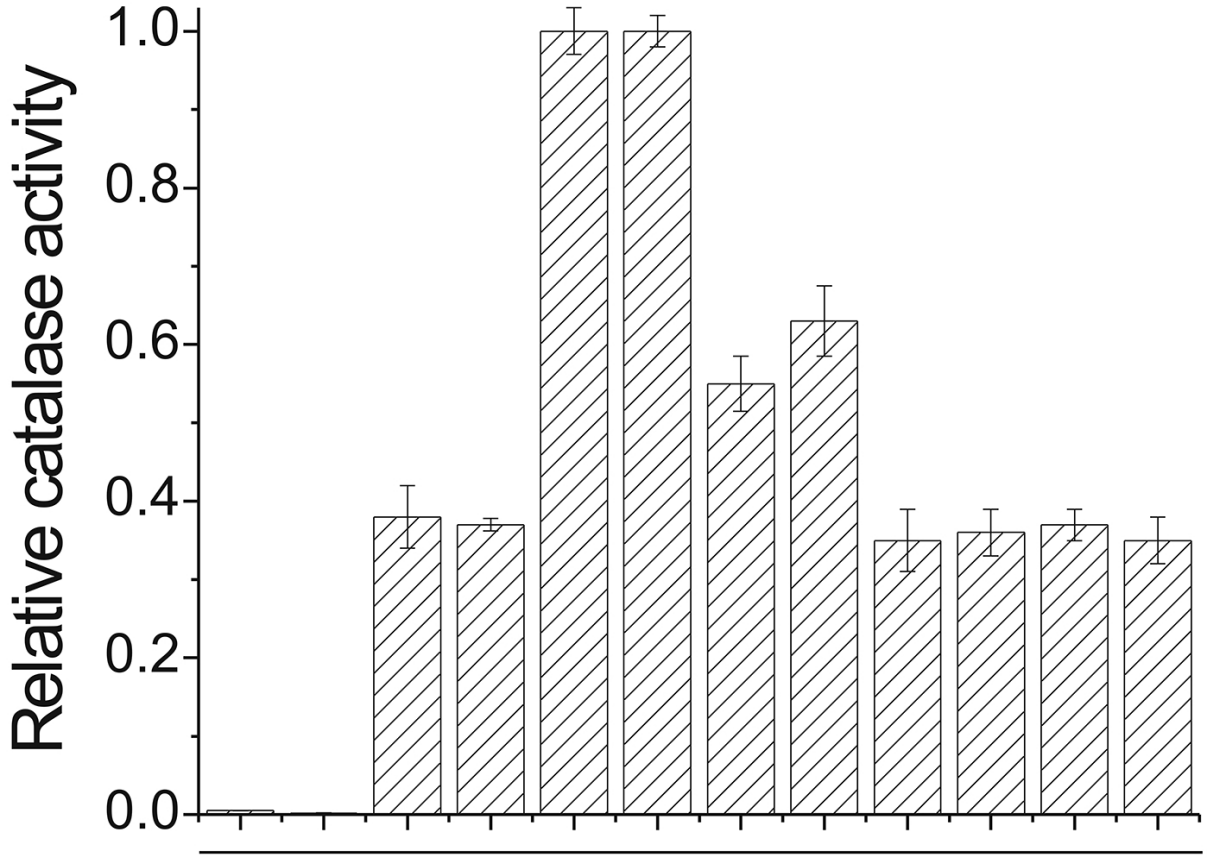

	1	2	3	4	5	6	7	8	9	10	11	12
GSH + Grx	✓		✓		✓		✓	✓				
NADPH + TrxR + Trx		✓		✓		✓			✓	✓	✓	✓
***Lin*catalase**			✓	✓	✓	✓	✓	✓	✓	✓	✓	✓
HClO treatment			✓	✓			✓	✓	✓	✓	✓	✓
0.25 μM *Lin*MsrB							✓					
0.5 μM *Lin*MsrB								✓				
0.25 μM *Lin*MsrA1									✓			
0.5 μM *Lin*MsrA1										✓		
0.25 μM *Lin*MsrA2											✓	
0.5 μM *Lin*MsrA2												✓

Figure 13

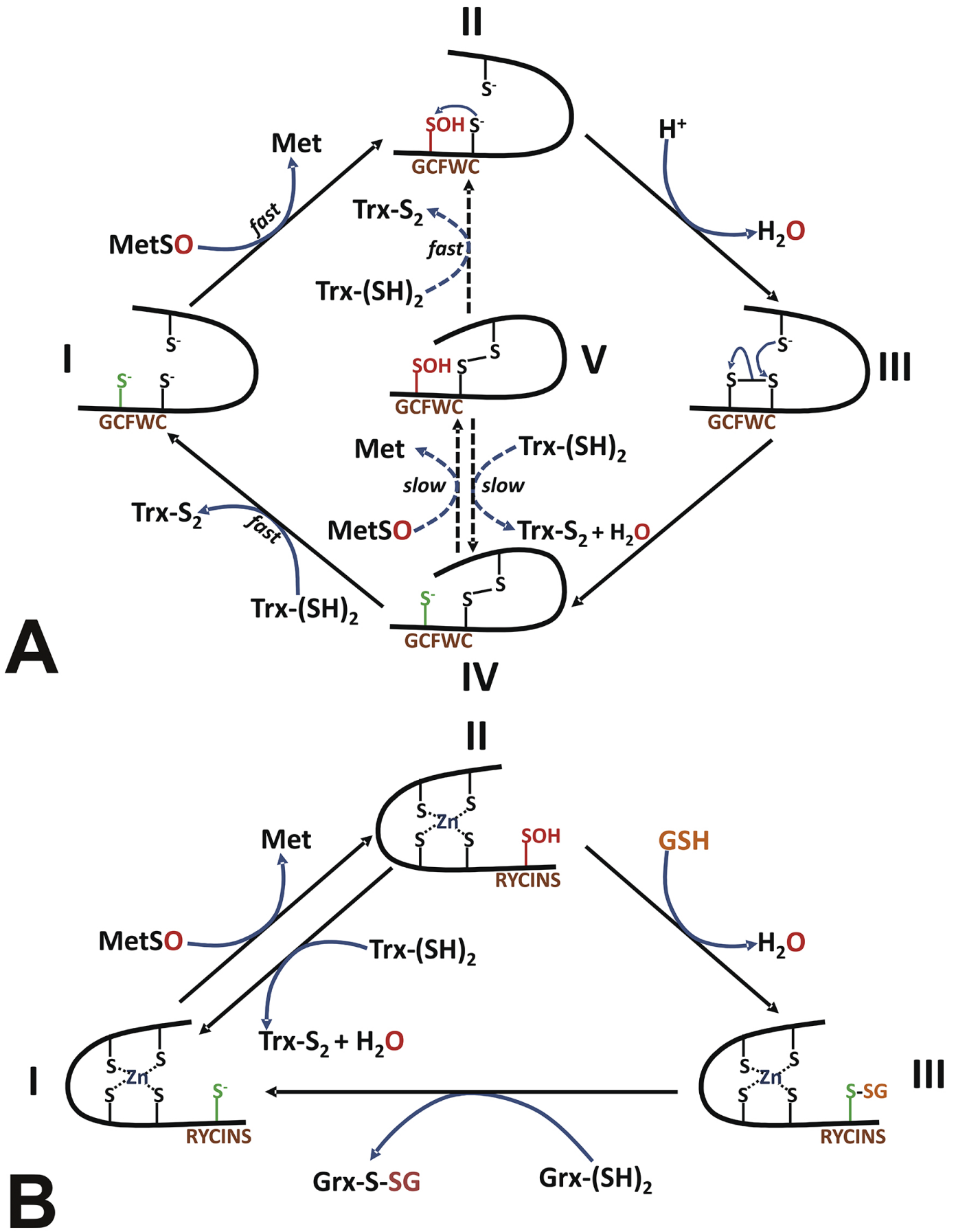
A
II
S-
SOH
S-
GCFWC
Met
fast
MetSO
Trx-S2
fast
Trx-(SH)2
H+
H2O
I
S-
S-
GCFWC
SOH
S
S
V
GCFWC
S-
S
S
III
GCFWC
Met
Trx-(SH)2
slow
slow
MetSO
Trx-S2 + H2O
Trx-S2
fast
Trx-(SH)2
S-
S
S
GCFWC
IV
B
II
S
Zn
S
S
S
SOH
RYCINS
Met
MetSO
Trx-(SH)2
Trx-S2 + H2O
GSH
H2O
I
S
Zn
S
S
S
S-
RYCINS
III
S
Zn
S
S
S
S-SG
RYCINS
Grx-S-SG
Grx-(SH)2

Figure 14